2012

Stability problems in constrained pendulum systems and time-delayed systems

Prashanth Ramachandran
Louisiana State University and Agricultural and Mechanical College, pramac1@lsu.edu

STABILITY PROBLEMS IN CONSTRAINED PENDULUM SYSTEMS AND TIME-DELAYED SYSTEMS

A Dissertation

Submitted to the Graduate Faculty of the
Louisiana State University and
Agricultural and Mechanical College
in partial fulfillment of the
requirements for the degree of
Doctor of Philosophy

in

The Department of Mechanical Engineering

by
Prashanth Ramachandran
B.E., Anna University, 2006
M.S., LSU, 2009
August 2012

I would like to dedicate this dissertation to my parents

Smt. Usha Rani Ramachandran

and

Shri. Ramachandran Parasuraman

for their unconditional support throughout my academic pursuits.

Acknowledgments

It would be rhetoric to say, “I sincerely appreciate the guidance of my advisor Dr. Yitshak Ram”. To be candid, I never thought, a doctorate was going to be a reality with me moving from Baton Rouge to Chicago to Houston, for my work. I owe a little too many for the motivation, passion for research, penchant for knowledge, professionalism and integrity, I imbibed from this man. The countless hours, I spent with him over my research and the conversations we shared are among the best of my graduate school experiences. He will always be a mentor and a friend for my life.

I would also like to extend my lavish appreciation to my advisor Dr. Marcio de Queiroz, who took me in during the final stages of my program and helped me cross the hurdle.

A word of appreciation is due for my committee members Dr. Su-Seng Pang, Dr. Michael Khonsari, Dr. Steve Cai and Dr. Joseph Giaime for evaluating my research.

I would like to thank all the faculty and staff members of the Department of Mechanical Engineering for making my graduate studies a thoroughly enjoyable exercise.

A family joke has been that “It takes a village to write a dissertation”. It does without skepticism, particularly with me working full time and doing research while writing this dissertation. My village would be incomplete without my parents and my brother Nishanth Ramachandran who have stood by me every way of the step regardless of my decisions.

Table of Contents

List of Tables

List of Figures

Abstract

In this dissertation, we study the boundary of stability of a class of linear mechanical systems as a function of a parameter. We consider two different systems under this class: a constrained double pendulum connected by a rigid rod and a state-feedback-controlled mechanical system with time delay. In the first system, the destabilizing parameter is the distance between the supports of the two pendulums. In the second system, the destabilizing parameter is the time delay.

In the constrained double pendulum system, linear perturbation analysis is used to determine the natural frequency of the system. Our analysis reveals a zone of instability in what seemingly is an inherently stable configuration. This *paradoxical* behavior, which is not mentioned in the literature until now, is explained and a simple experiment confirms the instability predicted by the analysis. The approach is extended to a chain of pendulums consisting of n masses and n+1 links, which is a lumped parameter model for small vibrations of a catenary. Our work confirms the existence of asymmetric stable equilibrium configurations for a symmetric system. The problem of determining the critical distance for instability between two supporting points of a catenary has potential application in the design of novel mechanical switches, sensors, and valves.

In the second part of the dissertation, we consider a linear mechanical system where a time delay exists in the linear state feedback control input. We seek a *closed-form solution* for the problem of determining the critical time delay for instability of the closed-loop system. Such a closed-form solution, which to the best of our knowledge is inexistent in the literature, offers an *exact* value for the critical time delay whereas a numerical solution is only approximate. We show that in the single-input/multi-output (SIMO) case of the class of systems under consideration, the problem may be reduced by using singular value decomposition to that of finding the roots of a certain polynomial. The obtained closed-form solution accurately predicts the smallest time delay that would render the SIMO system unstable when the control gain matrices have a unit rank. This technique however cannot be extended to the multi-input/multi-output case. Two numerical methods are therefore developed to solve this case. One method involves Newton's iterations and the other method involves bisection for multiple functions.

Chapter 1
Introduction

1.1 Overview of Dissertation

This dissertation is devoted to the problem of *determining the boundary of stability of a mechanical system as a function of a parameter*. More precisely, let the mechanical system have the following equation of motion in state-space form,

$$\dot{\mathrm{x}} = f\left(\mathrm{x}, \mathrm{u}, \upsilon\right) \tag{1.1}$$

where $\mathbf{x} = \begin{bmatrix}\mathbf{x}_1 & \mathbf{x}_2\end{bmatrix}^T$, $\mathbf{x}_1(t)$ is the position vector, $\mathbf{x}_2(t)$ is the velocity vector, $\mathbf{u}$ is the control vector, and υ is a constant scalar parameter that affects the system stability. The function $f\left(\mathrm{x}, \mathrm{u}, \upsilon\right)$ in (1.1) is given by

$$f\left(\mathrm{x}, \mathrm{u}, \upsilon\right) = \begin{bmatrix} \mathrm{x}_2 \\ -\mathrm{M}^{-1}\left(\mathrm{C}\mathrm{x}_2 + \mathrm{K}\mathrm{x}_1\right) + \mathrm{B}\mathrm{u} \end{bmatrix} \tag{1.2}$$

where **M** is a symmetric positive definite *mass* matrix, **C** and **K** are symmetric semi-positive definite *damping* and *stiffness* matrices, respectively, and **B** is the input matrix. We want to determine the critical parameter value υ_C for which (1.1)-(1.2) is on the verge of becoming unstable.

We consider two different systems that fall under this class of problems. In the first system, the potentially destabilizing parameter is the *distance* between the supports of two pendulums connected by a rod. In the second system, the parameter is the *time delay* in a state-feedback-controlled mechanical system. The double pendulum system is a special case of (1.2) where **C** and **u** are zero. On the other hand, the time-delayed system is a special case of (1.2) where the state feedback control law in (1.2) takes the form

$$\mathbf{u}(t-\tau) = \mathbf{F}^T\mathbf{x}_2(t-\tau) + \mathbf{G}^T\mathbf{x}_1(t-\tau) \tag{1.3}$$

where τ is the positive time delay, **F** and **G** are the control gain matrices.

In the double pendulum system, (1.2) is obtained after linearizing the original nonlinear dynamics about the equilibrium point of interest. The (local) stability of the equilibrium point is determined by the location of the poles of the linearized system model in the complex plane. We show that the system poles are a function of the parameter υ. Therefore, varying this parameter will cause the poles to move in the complex plane. The poles of the double pendulum system are confined to move on the imaginary axis, so the criterion for destabilization is having a pair of imaginary (complex conjugate) poles collide at the origin. In the time delay problem, the poles of the closed-loop system (1.1)-(1.3) move symmetrically about the real axis of the complex plane

due to their complex conjugate nature, so the criterion for destabilization is having a pair of imaginary poles of multiplicity two.

The organization and contributions of this dissertation are as follows. In Chapter 2, we discuss the stability problem of two pendulums connected by a rigid rod moving in a plane. Linear perturbation and eigenvalue analyses are used to determine the natural frequency of the system. The analysis reveals a counterintuitive phenomenon not found in the literature, viz., a zone of instability exists in what appears to be an inherently stable configuration of the double pendulum. This paradoxical behavior is resolved and a simple experiment confirms that the equilibrium position in the region indicated is unstable. Finally, the results are extended to a chain of pendulums consisting of n masses and $n+1$ links, which is a lumped parameter model for small vibrations of a catenary. The significance of this work is, first, that the result or merely the fact that such a pendulum system may be destabilized is interesting and novel. Second, the interpretation and the demonstration of the instability by a simple experiment have merit in engineering and physics education. Third, the phenomenon that increasing the distance between two points beyond a certain limit in one direction causes a sudden large tilt of links can be used in designing mechanical switches and sensing devices. These devices could be activated when the strain between two points exceeds a maximum allowable limit. Part of the work in Chapter 2 appeared in: P. Ramachandran, S. G. Krishna, and Y. M. Ram, "Instability of a constrained pendulum system", *American Journal of Physics*, Vol. 79 (4), pp. 395-400, Apr. 2011.

In Chapter 3, we consider the stability problem of a mechanical system with time delay in the state feedback control law. The practical application of measuring the state and actuating the system, may have an inherent time delay associated with it. This time delay between the instant of measurement of the state and the time of actuation can render the system unstable. In the event of instability, at least one of the eigenvalues $\lambda \equiv \alpha + i\beta$, of the transcendental eigenvalue problem has a positive real part, $\alpha > 0$. This chapter deals with the problem of determining a closed-form solution for the critical time delay where the system may lose or gain stability. It is well known from literature that the problem of finding a parameter τ and a repeated eigenvalue λ plays a crucial role in determining the stability of circulatory and continuous gyroscopic systems, such as buckling of columns by tangential forces and determining critical speeds in gyroscopic systems. It is remarkable that the problem of finding the critical time delay in mechanical controlled systems falls into this category. It is shown that for a single-input/multi-output (SIMO) system, the problem may be reduced by using singular value decomposition to one of finding the roots of a certain polynomial. This technique however cannot be extended to the MIMO system. Therefore two numerical methods, *Newton's iterations*, and *bisection for multiple functions*, are applied to analyze the stability for the MIMO case. The work in this chapter appeared in: P. Ramachandran, and Y. M. Ram, "Stability boundaries of mechanical controlled system with time delay", *Mechanical Systems and Signal Processing*, Vol. 27, pp. 523-533, Feb. 2012.

1.2 Background Theory

In this section, we review the basic concepts and mathematical tools used in studying the stability problems in Chapters 2 and 3.

1.2.1 Eigenvalue Problem

A gamut of problems in classical physics and mechanics, ranging from structural stability to vibration and control, fit into the class of *eigenvalue problem*. The generalized form of the eigenvalue problem is

$$(\mathbf{A} - \lambda\mathbf{B})\underline{\phi} = \mathbf{0} \tag{1.4}$$

where $\mathbf{A}$ and $\mathbf{B}$ are $n \times n$ matrices and $\underline{\phi}$ is a constant vector and λ is the eigenvalue.

The existence of a trivial solution $\underline{\phi} = \mathbf{0}$ for (1.5) is obvious and has no significance. The element of interest in an eigenvalue problem is the existence of non-trivial (non-zero) solutions. Taking stock that $\mathbf{A} - \lambda\mathbf{B}$ is a matrix, we cite the well-known result of linear algebra that a system of equations of the form $\mathbf{A} - \lambda\mathbf{B}$ has a unique solution if and only if $\mathbf{A}$ is non-singular.

Thus (1.5) has other non-trivial solutions provided $\mathbf{A} - \lambda\mathbf{B}$ is singular, i.e.,

$$\det(\mathbf{A} - \lambda\mathbf{B}) = 0 \tag{1.5}$$

1.2.2 The Concept of Stability

To illustrate the underlying idea of stability in dynamic systems, consider a single degree of freedom system composed of a particle m moving *without friction* along the parabola

$$y = \frac{1}{2}ax^2 \tag{1.6}$$

as shown in Figure 1.1, under the influence of its own weight mg.

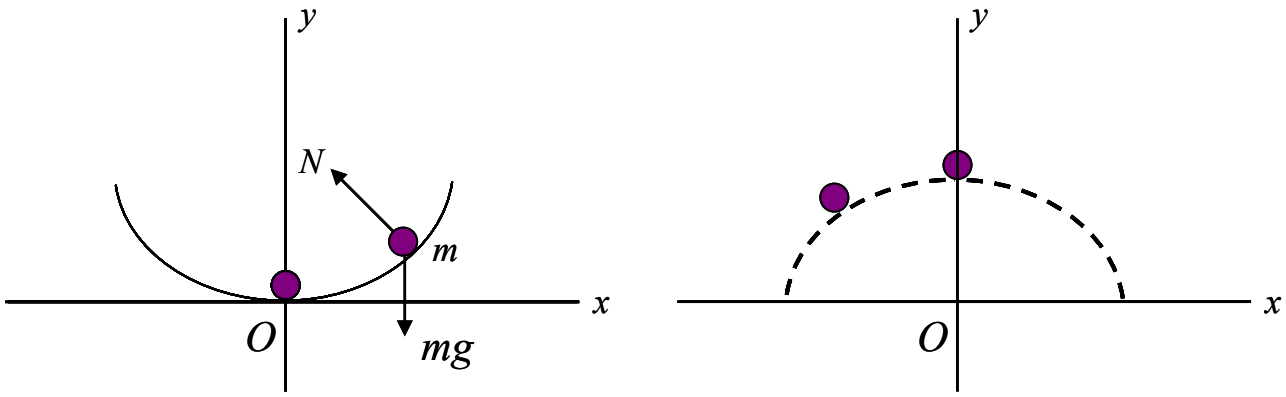

Figure 1.1 Particle moving on a parabola: (a) s*table* and (b) u*nstable* equilibria

The equilibrium position O with $a > 0$ is the only *stable equilibrium configuration* in the sense that small perturbations result in oscillations confined to the immediate vicinity of the equilibrium position. For $a < 0$, the position O is again the only equilibrium configuration, but it is *unstable*: an arbitrary small perturbation is followed by a rapid divergence of the particle position from O . The transition between stability and instability of the isolated equilibrium position O takes place when the parameter a vanishes. For $a = 0$, the parabola coincides with the $x-axis$ and an infinite number of equilibrium configurations corresponding to $x \neq 0$ appear as is the case in *neutral equilibrium*.

The location of poles provides a qualitative insight into the response characteristics of a system. In particular, the system poles directly define the components in the transient response. Linearizing (1.1) about an equilibrium point $\mathbf{x}_0$, we get

$$\delta\dot{\mathbf{x}} = \mathbf{A}(\upsilon)\delta\mathbf{x} \tag{1.7}$$

where $\delta\mathbf{x} = \mathbf{x} - \mathbf{x}_0$ is the state vector and $\mathbf{A}(\upsilon) = \partial f(\mathbf{x}, \upsilon)/\partial \mathbf{x}_{\mathbf{x}=\mathbf{x}_0}$ is the system matrix. The *local* stability of a linearized system is determined by the location of the eigenvalues of $\mathbf{A}$ on the complex plane. Figure 1.2 shows the form of homogenous response from the system pole locations.

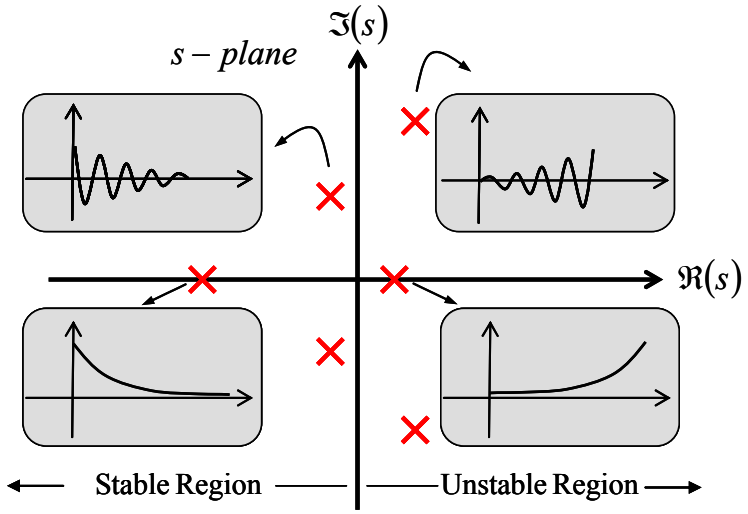

Figure 1.2 Response components of a system from pole locations

1. A real pole in the left-half of the complex plane defines an exponentially decaying component in the homogenous response. The rate of decay is determined by the real part of the pole; i.e., poles far from the origin in the left-half plane correspond to components that decay rapidly; while those near the origin correspond to a slowly decaying component.
2. A real pole in the right-half plane corresponds to an exponentially increasing component in the transient response; thus rendering the system unstable.
3. Complex conjugate pole pair in the left-half of the s - plane combine to generate a response with decaying oscillations.

4. A pole pair lying on the imaginary axis generates an oscillatory component with constant amplitude. A special case of this is a pole at the origin.
5. Repeated pole pairs on the imaginary axis or a complex pole pair on the right-half plane lead to a response with increasing oscillations.

1.2.3 State Feedback Control (Pole Placement)

State feedback in a mechanical system typically comprises of using the velocity and position measurements of the mass in a control law to provide the appropriate control signal. With the system defined by the state variable model as in Figure 1.3,

$$\dot{\mathbf{x}} = \mathbf{A}\mathbf{x} + \mathbf{B}\mathbf{u}, \tag{1.8}$$

we are particularly interested in controlling the system with a control signal $\mathbf{u}$ given by

$$\mathbf{u} = -\mathbf{F}\mathbf{x} = -\mathbf{F}_1\mathbf{x}_1 - \mathbf{F}_2\mathbf{x}_2, \tag{1.9}$$

where $\mathbf{x}_1$ is the position, $\mathbf{x}_2$ the velocity, and $\mathbf{F} = \begin{bmatrix}\mathbf{F}_1 & \mathbf{F}_2\end{bmatrix}$ is called the *gain*. The objective of (1.9) is to drive the state $\mathbf{x}(t)$ to zero.

Substituting (1.9) in (1.8) we obtain the closed-loop system

$$\dot{\mathbf{x}} = (\mathbf{A} - \mathbf{B}\mathbf{F})\mathbf{x} \tag{1.10}$$

The eigenvalue problem associated with (1.10), as discussed in Section 1.2.1, is

$$\det(\lambda\mathbf{I} - (\mathbf{A} - \mathbf{B}\mathbf{F})) = \mathbf{0} \tag{1.11}$$

A well-established method to assign the system poles at the desired locations for a single input system is the Ackermann's formula. This formula is given by

$$\mathbf{F} = \mathbf{e}_n\boldsymbol{\psi}^{-1}\mathbf{P}(A) \tag{1.12}$$

where $\mathbf{e}_n$ is a unit row vector with all elements 0 except the n^{th} element, which is 1, and

$$\boldsymbol{\psi} = \begin{bmatrix}\mathbf{B} & \mathbf{A}\mathbf{B} & \mathbf{A}^2\mathbf{B} & \ldots & \mathbf{A}^{n-1}\mathbf{B}\end{bmatrix}^T, \tag{1.13}$$

$$\mathbf{P}(s) = (s - p_1)\ldots(s - p_n) = s^n + \alpha_{n-1}s^{n-1} + \alpha_{n-2}s^{n-2} + \ldots\alpha_0 \tag{1.14}$$

Here, α_i are the coefficients of the monic polynomial

$$s^n + \alpha_{n-1}s^{n-1} + \alpha_{n-2}s^{n-2} + \ldots + \alpha_0 \tag{1.15}$$

and p_i's are the desired poles.

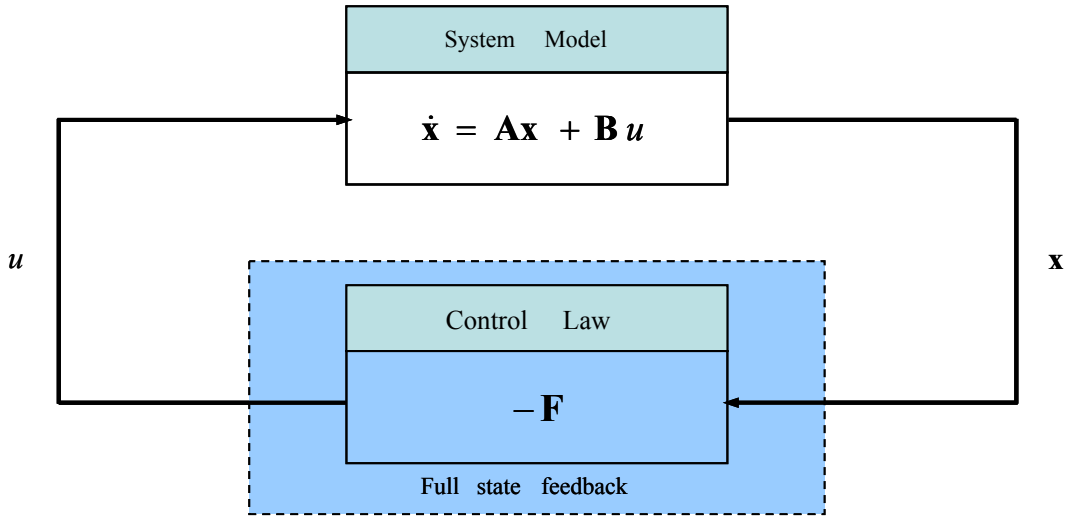

Figure 1.3 Block diagram of state feedback control

Chapter 2
Instability of a Constrained Pendulum System

The motion of a catenary is governed by a non-linear partial differential equation, where the non-linearity features in both the spatial and time variables. The modeling and response may be simplified considerably when the catenary is approximated by a chain of pendulums. Linear perturbation analysis is employed to gain insight in the case where the chain consists of two point masses and three rigid links. The results examined indicate a certain zone of instability in what looks like a stable system. The paradoxical phenomenon is explained and a simple experiment confirms the result.

2.1 Stability of a Catenary

At first glance, the dynamics of a catenary seem deceptively simple. It is true that very powerful numerical techniques exist today that could solve the most complicated cable problems, linear or nonlinear. Although the most fundamental properties of cables are well known, the theory of vibrations of suspended cables, supported at one or both ends, has been increasingly refined throughout the years. There is, however, an inadequacy in part of the theory which has apparently gone unnoticed or unresolved till now.

Stated briefly, the inadequacy has arisen because practically all previous theories that are valid for cables have centered around the analysis of continuous systems. Lagrange used a discrete string of beads model of the taut string as an illustration of the application of his equations of motion. At that time, however, the theory of partial differential equations was still in its infancy, and his work, among the first on the solution of vibration problems by difference equations, was done in 1760 and was included in his celebrated *Mecanique Analytique* of 1788.

Consider a uniform cable of length l and mass per unit length m that hangs in static equilibrium in a vertical plane through supports that are located at the same level as shown in Figure 2.1(a).

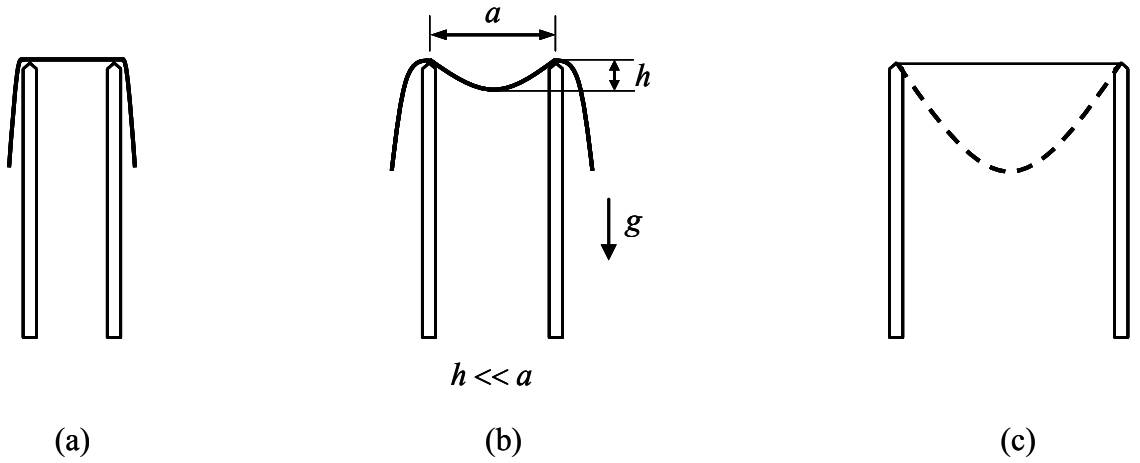

Figure 2.1 Configuration of the (a), (b) *stable equilibrium* and (c) *unstable* equilibrium

It is clear that the stable equilibrium configuration in Figure 2.1(b) becomes unstable and the cable falls due to its own weight as the ratio of sag h to span a is increased. At some ratio h/a, both the stable and the unstable equilibriums coincide. It is intuitive that the instability of the elastica will result in the cable slipping through and the supports failing to hold the cable. This can become a safety issue in construction sites and pipeline repair factories, in which the cable or pipe materials are stacked temporarily on supports.

Many researchers, both in the field of engineering and mathematics, have attempted to solve the stability problem of catenary systems with large deflection and have overlooked some critical phenomena. This chapter addresses the problem through linear perturbation analysis using discrete models. The results presented here, for which experimental confirmation has been obtained, are of considerable practical importance particularly in cases where the phenomenon of increasing the distance between two points beyond a certain limit in one direction causes a sudden large tilt of links. This phenomenon can be exploited to design mechanical switches and sensing devices. These devices could be activated when the strain between two points exceeds a maximum allowed level. Specifically, consider a scotch-yoke mechanism held in position by the weight of two pulleys and the distance between the cranks held by an electromagnet. During a power failure, the electromagnet is discharged resulting in an increase in the distance between the two points. Taking advantage of the instability, the large displacement to a stable equilibrium can be utilized in fail-closed valve (i.e., a valve that would go to a closed position on system failure).

2.2 Literature Review

An ordinary rigid planar pendulum suspended in the uniform gravitational field is a very useful and versatile physical model famous for its outstanding role in the history of physics. The pendulum is also interesting as a paradigm of contemporary nonlinear physics and, more importantly, because the differential equation of the pendulum is frequently encountered in various branches of modern physics. Thus, the pendulum is a rather simple classic nonlinear mechanical device, which models many physical systems and the analogies we gain provide an intuitive understanding of complex phenomena.

Irvine and Caughey (1974) developed a linear theory for the free vibrations of a uniform suspended cable in which the ratio of sag to span was about 1:8 or less. Both in-plane and out-of-plane motions were considered. It was shown that the analysis of the symmetric in-plane modes is heavily dependent on a parameter which allows for the effects of cable geometry and elasticity. Caldwell and Boyko (1991) explored the plausible linearization methods for a simple pendulum. The ‘equal-areas’ and the ‘minimax’ criteria were conferred and their unsuitability at extenuating circumstances were established.

The dynamics of a taut inclined cable with a riding accelerated mass was studied by Tadjbakhsh and Wang (1992) in which the dynamics of small deformations were superimposed on the static catenary state. It was shown that the problem of determining the natural frequencies of such a system may be decomposed into two parts: (a) determining the equilibrium configuration from the non-linear static equations, and then (b) *finding the dynamics of small deformations superimposed on the static state*.

Cromer (1994) approached the problem of many oscillations of a rigid rod – pendular, bifilar, torsional, coupled, nonlinear, and chaotic and provided interesting insights from an experimental and theoretical standpoint. The finite diameter of the pin upon which the rod oscillates was found to have an observable effect on the period. It was also shown from the energy integral method that the large angle oscillations of the bifilar pendulum departed by a measurable amount from the large angle oscillations of the physical pendulum.

Butikov (2001) showed that when the frequency and/or amplitude of vibration of the suspension point of an inverted pendulum that is constrained to vibrate along the vertical line is large enough, the inverted pendulum shows no tendency to turn down. The physical reason for this phenomenon was shown to be that the mean torque of the force of inertia is greater than the torque of the force of gravity at rapid oscillations. An effective potential function for the pendulum with the axis vibrating at a high frequency was developed and the upper boundary of the dynamic stability was investigated. Finally, the behavior of the parametrically-excited pendulum with its nonlinear large-amplitude motions was showcased.

Rafat, Wheatland, and Bedding (2008) investigated a variation of the simple double pendulum in which the two point masses were replaced by square plates. The equations of motion obtained using the Lagrangian formalism followed by an analysis of its behavior at different energy ranges, i.e., low and high energy exhibited a richer behavior than the simple double pendulum and provided a convenient demonstration of nonlinear dynamics and chaos. Maianti, Pagliara, Galimberti, and Parmigiani (2009) extended the work of Cadwell and Boyko by describing the mechanics of two pendulums coupled by a stressed spring. For small oscillations, it was found that the system at its highest symmetry configuration rendered the two pendulums independent and that the normal frequencies degenerate.

Chen, Li, and Ro (2009) conducted a linear stability analysis of a heavy flexible beam resting on frictionless point supports. A dynamic analysis was conducted in order to determine the nature of stability of various equilibrium configurations and the corresponding natural frequencies. It was concluded that a stable equilibrium exists only when the support span is within a range of a dimensionless ratio between the weight density and the flexural rigidity of the elastica. When the span decreased beyond the minimum value, the elastica slipped away from the side, and on the other hand, when the span increased, the elastica slipped through between the two supports.

2.3 Equations of Motion of a Largely-Deflected Double Pendulum System

The constrained double-pendulum system consists of two point masses m, pin-connected by three inflexible weightless links of lengths l, as shown in Figure 2.2(a). The distance between the pivots O_A and O_B of the pendula is Δ, the gravitational field is g, and the angles $\theta_k(t)$, $k = 1,2,3$, of the links from the vertices are defined in the figure. For convenience we define a dimensionless distance $d = \Delta/l$. It is clear from Figure 2.2(a) that $-1 < d < 3$; $d < 0$ indicates that the two links cross each other such that the pivot point O_B is to the left of pivot O_A. Figure 2.2(b) shows the system in a stable equilibrium position. The static angles ϑ_k of the links are defined in the figure.

Considering the in-plane motion of the system, the potential energy of the dynamic system in Figure 2.2(a) is

$$\begin{aligned} V_1 &= mgl\left(-\cos\theta_1 - \cos\theta_1 - \cos\theta_2\right) \\ &= mgl\left(2\cos\theta_1 + \cos\theta_2\right) \end{aligned} \tag{2.1}$$

The potential energy of the static system in Figure 2.2(b) is

$$\begin{aligned} V_2 &= mgl\left(-\cos\vartheta_1 - \cos\vartheta_1 - \cos\vartheta_2\right) \\ &= mgl\left(2\cos\vartheta_1 + \cos\vartheta_2\right) \end{aligned} \tag{2.2}$$

The change in potential energy of the system is thus

$$\begin{aligned} V &= V_2 - V_1 \\ &= mgl\left(2\cos\vartheta_1 + \cos\vartheta_2 - 2\cos\theta_1 - \cos\theta_2\right) \end{aligned} \tag{2.3}$$

while the kinetic energy takes the form

$$\begin{aligned} T &= \frac{1}{2}m\left[\left(l\cos\theta_1\dot{\theta}_1\right)^2 + \left(l\sin\theta_1\dot{\theta}_1\right)^2 + \left(l\cos\theta_1\dot{\theta}_1 + l\cos\theta_2\dot{\theta}_2\right)^2 + \left(l\sin\theta_1\dot{\theta}_1 + l\sin\theta_2\dot{\theta}_2\right)^2\right] \\ &= \frac{1}{2}ml^2\left(2\dot{\theta}_1^2 + \dot{\theta}_2^2 + 2\dot{\theta}_1\dot{\theta}_2\cos\left(\theta_2 - \theta_1\right)\right) \end{aligned} \tag{2.4}$$

The constraints are

$$\phi_1 = l\left(\sin\theta_1 + \sin\theta_2 + \sin\theta_3\right) - \Delta = 0 \tag{2.5}$$

and

$$\phi_2 = l\left(\cos\theta_1 + \cos\theta_2 + \cos\theta_3\right) = 0 \tag{2.6}$$

implying, that the horizontal and vertical distances between O_A and O_B are Δ and zero, respectively.

The Lagrangian associated with the problem is

$$L = T - V - \hat{\lambda}mg\phi_1 - \hat{\mu}mg\phi_2 \tag{2.7}$$

where $\hat{\mu}$ and $\hat{\lambda}$ are time dependent Lagrange multipliers. The Lagrange multipliers are the physical measures that impose the constraint on the system.

The motion of the system is determined by the Euler-Lagrange equations

$$\frac{\partial L}{\partial \theta_k} - \frac{d}{dt}\frac{\partial L}{\partial \dot{\theta}_k} = 0\,, \qquad k = 1,2,3 \tag{2.8}$$

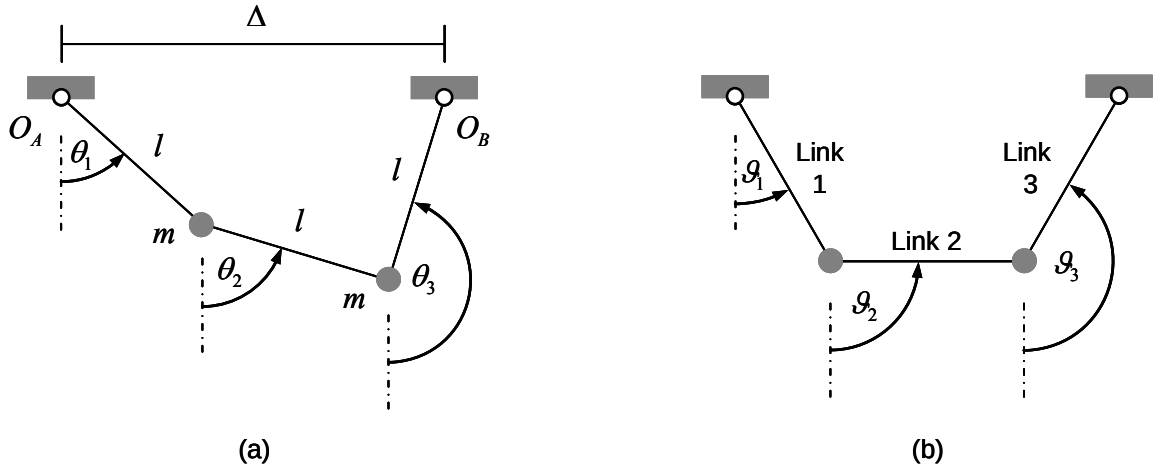

Figure 2.2 Definition of the (a) dynamic and (b) static configurations

For $k = 1$, we obtain

$$\frac{\partial L}{\partial \theta_1} = ml^2\left(\dot{\theta}_1\dot{\theta}_2 \sin(\theta_2 - \theta_1)\right) - 2mgl\sin\theta_1 - \hat{\lambda}mgl\cos\theta_1 + \hat{\mu}mgl\sin\theta_1$$

$$\frac{\partial L}{\partial \dot{\theta}_1} = ml^2\left(2\dot{\theta}_1 + \dot{\theta}_2\cos(\theta_2 - \theta_1)\right)$$

$$\frac{d}{dt}\frac{\partial L}{\partial \dot{\theta}_1} = ml^2\left(2\ddot{\theta}_1 - \dot{\theta}_2\sin(\theta_2 - \theta_1)(\dot{\theta}_2 - \dot{\theta}_1) + \ddot{\theta}_2\cos(\theta_2 - \theta_1)\right)$$

$$\begin{aligned}\Rightarrow \frac{\partial L}{\partial \theta_1} - \frac{d}{dt}\frac{\partial L}{\partial \dot{\theta}_1} &= l\left(2\ddot{\theta}_1 + \ddot{\theta}_2\cos(\theta_2 - \theta_1) - \dot{\theta}_2^2\sin(\theta_2 - \theta_1)\right) \\ &\quad - (\hat{\mu} - 2)g\sin\theta_1 + \hat{\lambda}g\cos\theta_1 = 0\end{aligned} \tag{2.9a}$$

Differentiating similarly for $k = 2,3$, we obtain

$$\begin{aligned}\frac{\partial L}{\partial \theta_2} - \frac{d}{dt}\frac{\partial L}{\partial \dot{\theta}_2} &= l\left(\ddot{\theta}_2 + \ddot{\theta}_1\cos(\theta_1 - \theta_2) - \dot{\theta}_1^2\sin(\theta_1 - \theta_2)\right) \\ &\quad - (\hat{\mu} - 1)g\sin\theta_2 + \hat{\lambda}g\cos\theta_2 = 0\end{aligned} \tag{2.9b}$$

$$\frac{\partial L}{\partial \theta_3} - \frac{d}{dt}\frac{\partial L}{\partial \dot{\theta}_3} = -\hat{\mu}g\sin\theta_3 + \hat{\lambda}g\cos\theta_3 = 0 \tag{2.9c}$$

The system of equations (2.5), (2.6) and (2.9) consists of five equations with five unknowns: $\theta_k(t)$, $k=1,2,3$, which determine the dynamics of the three links, and $\hat{\lambda}(t)$, $\hat{\mu}(t)$ the two Lagrange multipliers. The stability parameter Δ as described in (2.5) determines the configuration and response characteristics of the system.

2.3.1 Equations of Static Equilibrium

The equations of static equilibrium are trivially obtained from their dynamic counterparts, (2.9), (2.5), and (2.6), by omitting time derivative terms and substituting ϑ_k for θ_k, μ for $\hat{\mu}$ and λ for $\hat{\lambda}$

$$\begin{cases} (2-\mu)\sin\vartheta_1 + \lambda\cos\vartheta_1 = 0 \\ (1-\mu)\sin\vartheta_2 + \lambda\cos\vartheta_2 = 0 \\ -\mu\sin\vartheta_3 + \lambda\cos\vartheta_3 = 0 \\ \sin\vartheta_1 + \sin\vartheta_2 + \sin\vartheta_3 = d \\ \cos\vartheta_1 + \cos\vartheta_2 + \cos\vartheta_3 = 0 \end{cases} \tag{2.10}$$

The equations in (2.10) have the closed form solution

$$\vartheta_1 = \sin^{-1}\frac{D-1}{2}, \quad \vartheta_2 = \frac{\pi}{2}, \quad \vartheta_3 = \pi - \vartheta_1, \quad \mu = 1, \quad \lambda = -\tan\vartheta_1, \tag{2.11}$$

corresponding to the configuration of static equilibrium shown in Figure 2.2(b).

2.4 Linearized Equations of Motion

To describe small oscillations about the equilibrium position, we denote

$$\theta_k(t) = \vartheta_k + \varepsilon_k(t),\ k=1,2,3, \quad \hat{\mu} = \mu + \varepsilon_\mu(t), \quad \hat{\lambda} = \lambda + \varepsilon_\lambda(t) \tag{2.12}$$

where ε_k, ε_μ, and ε_λ are infinitesimal quantities. The parameters in (2.12) are substituted in (2.9), the static equations in (2.10) are subtracted from the results, and the higher-order terms in ε are eliminated to obtain the linearized equations of motion.

Consider (2.9c),

$$-\hat{\mu}g\sin\theta_3 + \hat{\lambda}g\cos\theta_3 = 0$$

Substituting

$$\theta_3 = \vartheta_3 + \varepsilon_3, \quad \hat{\mu} = \mu + \varepsilon_\mu, \quad \hat{\lambda} = \lambda + \varepsilon_\lambda$$

we obtain

$$-g(\mu+\varepsilon_\mu)\sin(\vartheta_3+\varepsilon_3)+g(\lambda+\varepsilon_\lambda)\cos(\vartheta_3+\varepsilon_3)=0$$

Since $\sin\varepsilon_3=\varepsilon_3$, $\cos\varepsilon_3=1$ for small oscillations, the above equation reduces to,

$$-g(\mu+\varepsilon_\mu)(\sin\vartheta_3+\varepsilon_3\cos\vartheta_3)+g(\lambda+\varepsilon_\lambda)(\cos\vartheta_3-\varepsilon_3\sin\vartheta_3)=0$$

Subtracting the static equations from above and simplifying yields,

$$\{-g(\mu+\varepsilon_\mu)(\sin\vartheta_3+\varepsilon_3\cos\vartheta_3)+g(\lambda+\varepsilon_\lambda)(\cos\vartheta_3-\varepsilon_3\sin\vartheta_3)\}$$
$$-\{-\mu g\sin\vartheta_3+\lambda g\cos\vartheta_3\}=0$$

$$\Rightarrow -g\mu\sin\vartheta_3-g\mu\varepsilon_3\cos\vartheta_3-g\varepsilon_\mu\sin\vartheta_3-g\varepsilon_\mu\varepsilon_3\cos\vartheta_3+g\lambda\cos\vartheta_3$$
$$-g\lambda\varepsilon_3\sin\vartheta_3+g\varepsilon_\lambda\cos\vartheta_3-g\varepsilon_\lambda\varepsilon_3\sin\vartheta_3+\mu g\sin\vartheta_3-\lambda g\cos\vartheta_3=0$$

Neglecting higher-order terms

$$-g\varepsilon_\mu\varepsilon_3\cos\vartheta_3-g\varepsilon_\lambda\varepsilon_3\sin\vartheta_3$$

$$=-g\mu\sin\vartheta_3-g\mu\varepsilon_3\cos\vartheta_3-g\varepsilon_\mu\sin\vartheta_3+g\lambda\cos\vartheta_3-g\lambda\varepsilon_3\sin\vartheta_3$$
$$+g\varepsilon_\lambda\cos\vartheta_3+\mu g\sin\vartheta_3-\lambda g\cos\vartheta_3=0$$
$$=-g\mu\varepsilon_3\cos\vartheta_3-g\varepsilon_\mu\sin\vartheta_3-g\lambda\varepsilon_3\sin\vartheta_3+g\varepsilon_\lambda\cos\vartheta_3=0$$
$$=-g\varepsilon_3(\lambda\sin\vartheta_3+\mu\cos\vartheta_3)+g(\varepsilon_\lambda\cos\vartheta_3-\varepsilon_\mu\sin\vartheta_3)=0$$

Thus, the linearized equations of motion for (2.9) are

$$\begin{cases} l(2\ddot{\varepsilon}_1+\ddot{\varepsilon}_2\cos(\theta_2-\theta_1))-\varepsilon_1 g(\lambda\sin\vartheta_1+(\mu-2)\cos\vartheta_1)+g(\varepsilon_\lambda\cos\vartheta_1-\varepsilon_\mu\sin\vartheta_1)=0 \\ l(\ddot{\varepsilon}_2+\ddot{\varepsilon}_1\cos(\theta_1-\theta_2))-\varepsilon_2 g(\lambda\sin\theta_2+(\mu-1)\cos\vartheta_2)+g(\varepsilon_\lambda\cos\theta_2-\varepsilon_\mu\sin\vartheta_2)=0 \\ -\varepsilon_3 g(\lambda\sin\vartheta_3+\mu\cos\vartheta_3)+g(\varepsilon_\lambda\cos\vartheta_3-\varepsilon_\mu\sin\vartheta_3)=0 \end{cases} \quad (2.13)$$

Linearization of the constraints gives

$$\varepsilon_1\cos\vartheta_1+\varepsilon_2\cos\vartheta_2+\varepsilon_3\cos\vartheta_3=0 \quad (2.14)$$

and

$$-\varepsilon_1\sin\vartheta_1-\varepsilon_2\sin\vartheta_2-\varepsilon_3\sin\vartheta_3=0 \quad (2.15)$$

by virtue of (2.5) and (2.6).

The linear system of equations (2.13), (2.14), and (2.15) may be written in matrix form

$$\mathbf{M}\ddot{\boldsymbol{\varepsilon}} + \mathbf{K}\boldsymbol{\varepsilon} = \mathbf{0}, \tag{2.16}$$

where

$$\boldsymbol{\varepsilon} = \begin{pmatrix} \varepsilon_1 & \varepsilon_2 & \varepsilon_3 & \varepsilon_\lambda & \varepsilon_\mu \end{pmatrix}^T, \tag{2.17}$$

$$\mathbf{K} = g\begin{bmatrix} \kappa_{11} & 0 & 0 & \cos\vartheta_1 & -\sin\vartheta_1 \\ 0 & \kappa_{22} & 0 & \cos\vartheta_2 & -\sin\vartheta_2 \\ 0 & 0 & \kappa_{33} & \cos\vartheta_3 & -\sin\vartheta_3 \\ \cos\vartheta_1 & \cos\vartheta_2 & \cos\vartheta_3 & 0 & 0 \\ -\sin\vartheta_1 & -\sin\vartheta_2 & -\sin\vartheta_3 & 0 & 0 \end{bmatrix}, \tag{2.18}$$

$$\kappa_{ii} = \big((3-i)-\mu\big)\cos\vartheta_i - \lambda\sin\vartheta_i, \qquad i = 1,2,3, \tag{2.19}$$

$$\mathbf{M} = l\begin{bmatrix} 2 & \cos(\vartheta_2-\vartheta_1) & 0 & 0 & 0 \\ \cos(\vartheta_1-\vartheta_2) & 1 & 0 & 0 & 0 \\ 0 & 0 & 0 & 0 & 0 \\ 0 & 0 & 0 & 0 & 0 \\ 0 & 0 & 0 & 0 & 0 \end{bmatrix}. \tag{2.20}$$

It is not difficult to show that (2.16) is equivalent to (1.1) and (1.2) when $\mathbf{C} = 0$ and $\mathbf{u} = 0$.

The double pendulum system represents a classical case of determining the stability boundaries as a function of a parameter in the degenerate case of an uncontrolled-undamped system. The solution of (2.16) takes the form

$$\boldsymbol{\varepsilon}(t) = \mathbf{v}e^{st} \tag{2.21}$$

where s defines the system poles.

Substituting (2.21) in (2.16) gives

$$\left(s^2\mathbf{M} + \mathbf{K}\right)\mathbf{v} = \mathbf{0} \tag{2.22}$$

It is well known that the poles of a polynomial with real coefficients are either purely real or appear in complex conjugate pairs. The existence of a single complex pole without a corresponding conjugate pole would generate complex co-efficients in the polynomial. The matrix $\mathbf{M}$ is symmetric positive definite and $\mathbf{K}$ is symmetric semi-positive definite. The stability boundary associated with (2.22) is determined by the condition that the real part of s

vanishes. But when the system is marginally stable, the poles of (2.22) are inherently imaginary. This implies that destabilization by a structural parameter may occur, when the roots belonging to two distinct pairs meet on the imaginary axis and then move away from the axis. In otherwords, the system is on its stability boundary when two poles collide on the imaginary axis, i.e. the property of double symmetry.

Theorem 1

The poles of (2.22) have double symmetry, i.e., they are *symmetric about the real and imaginary axes* of the complex plane.

Proof

The proof comprises 2 parts. Let us first prove that the poles are symmetric about the real axis.

Suppose that

$$s = \alpha + i\beta \qquad \mathbf{v} = \boldsymbol{\mu} + i\boldsymbol{\psi} \tag{2.23}$$

is a matrix pencil of (2.22). Substituting (2.23) in (2.22) gives

$$\left(\left(\alpha + i\beta\right)^2 \mathbf{M} + \mathbf{K}\right)\left(\boldsymbol{\mu} + i\boldsymbol{\psi}\right) = \mathbf{0} \tag{2.24}$$

Separating the real and imaginary parts, we obtain

$$\left(\left(\alpha^2 - \beta^2\right)\mathbf{M} + \mathbf{K}\right)\boldsymbol{\mu} - \left(2\alpha\beta\mathbf{M}\right)\boldsymbol{\psi} = \mathbf{0} \tag{2.25}$$

and

$$i\left(2\alpha\beta\mathbf{M}\right)\boldsymbol{\mu} + \left(\left(\alpha^2 - \beta^2\right)\mathbf{M} + \mathbf{K}\right)\left(i\boldsymbol{\psi}\right) = \mathbf{0} \tag{2.26}$$

We will now show that,

$$\bar{s} = \alpha - i\beta \qquad \bar{\mathbf{v}} = \boldsymbol{\mu} - i\boldsymbol{\psi} \tag{2.27}$$

is a matrix pencil of (2.22) as well.

Substituting (2.27) in (2.22) gives

$$\left(\left(\alpha - i\beta\right)^2 \mathbf{M} + \mathbf{K}\right)\left(\boldsymbol{\mu} - i\boldsymbol{\psi}\right) = \mathbf{0} \tag{2.28}$$

Separating the real and imaginary parts, we get

$$\left(\left(\alpha^2 - \beta^2\right)\mathbf{M} + \mathbf{K}\right)\boldsymbol{\mu} - \left(2\alpha\beta\mathbf{M}\right)\boldsymbol{\psi} = \mathbf{0} \tag{2.29}$$

and

$$i(-2\alpha\beta\mathbf{M})\boldsymbol{\mu} - \left((\alpha^2 - \beta^2)\mathbf{M} + \mathbf{K}\right)(i\boldsymbol{\psi}) = \mathbf{0} \tag{2.30}$$

by virtue of (2.25) and (2.26). It thus follows that if s is an eigenvalue of (2.22) so is $\bar{s}$, i.e., the eigenvalues are symmetric about the x axis.

Let us now prove that the poles are indeed symmetric about the imaginary axis as well i.e., $-s$ and $\mathbf{v}$ satisfy (2.22) as well.

Substituting $-s$ in lieu of s gives

$$\left((-s)^2\mathbf{M} + \mathbf{K}\right)\mathbf{v} = \left(s^2\mathbf{M} + \mathbf{K}\right)\mathbf{v} = \mathbf{0}\,. \tag{2.31}$$

by virtue of (2.22). The poles of (2.22) therefore have the double symmetry property; they are symmetric about the real and the imaginary axis. Furthermore, when the system is degenerated in the sense that it has only one degree of freedom, the two poles necessarily collide at the origin of the complex plane, i.e., $s = 0$. ■

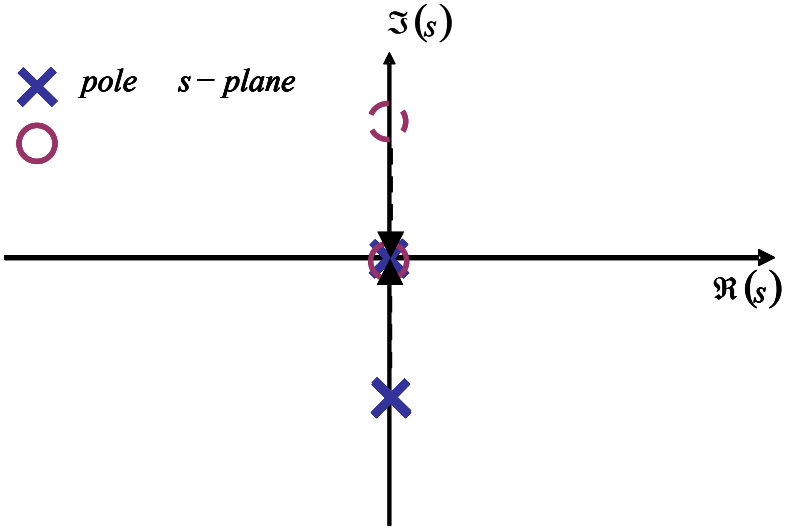

Fig 2.3 Property of d*ouble symmetry* for a single degree of freedom system

Note that in forming $\mathbf{K}$ in (2.18), the homogenous constraints (2.14) and (2.15) were multiplied by g. It thus follows from the formulation (2.16)-(2.20) that, similar to the vibrations of a simple pendulum, the natural frequency of small oscillations in the double pendulum is independent of the mass m and is proportional to $\sqrt{g/l}$.

Using separation of variables, the solution of (2.16) takes the form

$$\boldsymbol{\varepsilon}(t) = \mathbf{v}\sin\omega t \tag{2.32}$$

where $\mathbf{v}$ is a constant vector. Substituting (2.32) in (2.16) gives a standard eigenvalue problem

$$\left(\mathbf{K}-\omega^2\mathbf{M}\right)\mathbf{v}=\mathbf{0}. \tag{2.33}$$

From the solution of the equations of static equilibrium given by (2.11), equations (2.18)-(2.20) are simplified to

$$\mathbf{K}=g\begin{bmatrix} 1/\cos\vartheta_1 & 0 & 0 & \cos\vartheta_1 & -\sin\vartheta_1 \\ 0 & -\tan\vartheta_1 & 0 & 0 & -1 \\ 0 & 0 & 1/\cos\vartheta_1 & -\cos\vartheta_1 & -\sin\vartheta_1 \\ \cos\vartheta_1 & 0 & -\cos\vartheta_1 & 0 & 0 \\ -\sin\vartheta_1 & -1 & -\sin\vartheta_1 & 0 & 0 \end{bmatrix} \tag{2.34}$$

and

$$\mathbf{M}=l\begin{bmatrix} 2 & \sin\vartheta_1 & 0 & 0 & 0 \\ \sin\vartheta_1 & 1 & 0 & 0 & 0 \\ 0 & 0 & 0 & 0 & 0 \\ 0 & 0 & 0 & 0 & 0 \\ 0 & 0 & 0 & 0 & 0 \end{bmatrix}. \tag{2.35}$$

The eigenvalue problem (2.33) with $\mathbf{K}$ and $\mathbf{M}$ given by (2.34) and (2.35) has one finite eigenpair

$$\omega^2=\frac{1+2\sin^3\vartheta_1}{\cos\vartheta_1}\frac{g}{l}, \tag{2.36}$$

$$\mathbf{v}=\varepsilon_1\begin{pmatrix}1 & -2\sin\vartheta_1 & 1 & \left(1+2\sin^3\vartheta_1\right) & \left(\tan\vartheta_1-2\cos\vartheta_1\sin^2\vartheta_1\right)\end{pmatrix}^T \tag{2.37}$$

2.5 Stable and Unstable Position of a Largely-Deflected Double Pendulum System

The range of possible distance between the pivot points O_A and O_B is $-1<d<3$, where negative d indicates that the pivot O_B is on the left hand side of O_A. In such a case, Link 1 and Link 3 cross each other, as in Figure 2.6. Figure 2.4 shows the frequency equation (2.36) plotted versus d.

2.5.1 Natural Frequency of a Simple Pendulum

When $d = 1$, the slope of Link 1 in the static position is $\vartheta_1 = 0$. The frequency equation (2.36) gives for this case $\omega^2 = g/l$. This is an anticipated result since both pendulums, the one consisting of Link 1 with its attached mass and the one consisting of Link 3 with its attached mass, vibrates individually with a common natural frequency $\omega = \sqrt{g/l}$. The role of connecting Link 2 is limited to synchronizing the motion of the two pendula and not to average their frequency of oscillations.

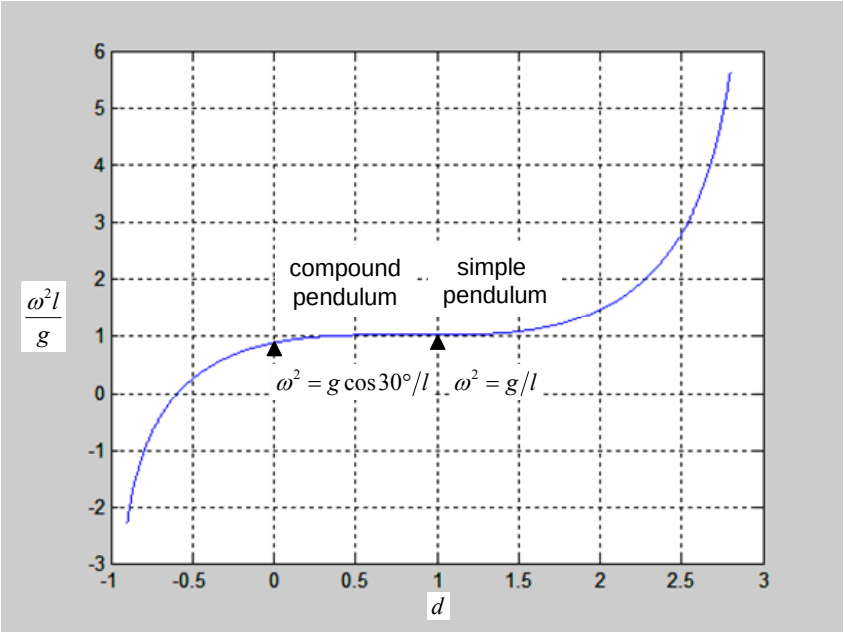

Figure 2.4 Graph of ω^2 versus d.

2.5.2 Natural Frequency of a Physical Pendulum

When $d = 0$, the slope of Link 1 in the static position is $\vartheta_1 = -\pi/6$ and (2.36) gives

$$\omega^2 = \frac{g}{l}\cos(\pi/6) \tag{2.38}$$

In this case, the double pendulum system is reduced to the physical pendulum shown in Figure 2.5.

The natural frequency of the physical pendulum is

$$\omega = \sqrt{\frac{Mg\rho}{I}} \tag{2.39}$$

where M is the total mass of the physical pendulum, ρ is the distance between the pivot O and the center of gravity G, and I is the moment of inertia of the pendulum about its pivot O. For the physical pendulum of Figure 2.5, $M = 2m$, $\rho = l\cos(\pi/6)$ and $I = 2ml^2$. Substituting these values in (2.39) gives (2.38).

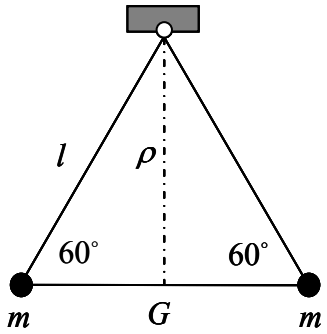

Figure 2.5 The physical pendulum obtained when $d = 0$.

2.5.3 The Paradox

Note that the frequency graph in Figure 2.4 indicates that ω^2 is negative in certain region. This implies that in this range there are no oscillations about equilibrium. More precisely, the frequency graph implies that the system is unstable when

$$d < d_{CR} = 1 - 2^{2/3} \cong -0.5874, \tag{2.40}$$

where d_{CR} is the critical distance of d that separates the zone of stable and unstable motion. When $d = d_{CR}$ the corresponding angle of static equilibrium for Link 1 is

$$\vartheta_1\big|_{d=d_{CR}} = \sin^{-1}\left(-0.5^{1/3}\right) \cong -52° \tag{2.41}$$

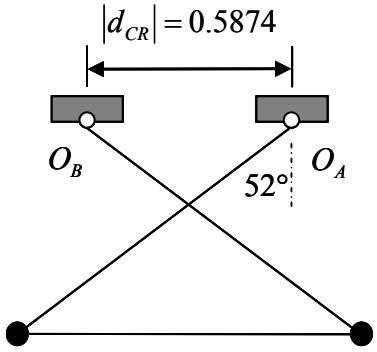

Figure 2.6 Configuration of the system when $d = d_{CR}$

by virtue of Equation (2.11). The configuration of the double pendulum system for this case, on its right proportions, is shown in Figure 2.6.

At glance, it appears that such a configuration is stable. Could it be possible that the linear perturbation analysis failed to properly characterize the physical behavior of the system? A system with no stable equilibrium state would consist of a *perpetuum mobile*.

2.5.4 The Paradox Resolved

Let us accept the results of the linear perturbation analysis and assume that when $d < d_{CR}$ the static configuration of the pendulum system with horizontal Link 2 is unstable. Then, a small perturbation will cause the system to move to a stable static configuration and to oscillate about it.

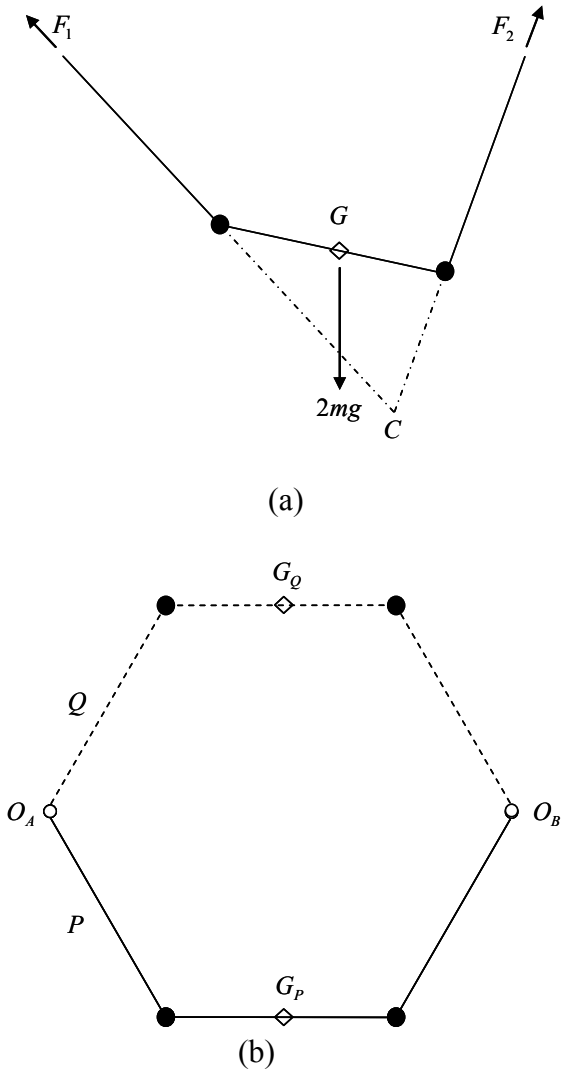

Figure 2.7 (a) Free body diagram and (b) possible static equilibrium positions.

If our intuition regarding stability did not mislead us entirely, and the system is not strongly unstable, then when d is slightly smaller than d_{CR}, the stable static position should be in the neighborhood of the unstable configuration with horizontal Link 2.To examine this hypothesis we inspect the free-body-diagram for $d > 1$ shown in Figure 2.7(a). If the system is in static equilibrium then the sum of the moments of all external forces about any point should vanish. Let C be the intersection of the extensions of Link 1 and Link 3 and let G be the center of gravity for the pendulum system, i.e., G is the mid-point of Link 2, as shown in the figure.

Since moment summation about C vanishes only when G is aligned vertically with point C it follows that a necessary condition for static equilibrium is that C lies directly above or below G. This implies that the only possible static equilibrium positions when $d > 0$ are when Link 2 is horizontal, i.e., the lower configuration P or the upper configuration Q, shown in Figure 2.7(b).

But when $d < d_{CR}$, it is possible that there is a non-symmetric static equilibrium. We solved the static equilibrium equations (2.10) for the case $d = -0.6$ and found the two neighboring solutions, listed in Table 2.1. The configurations associated with these solutions, labeled P and Q, are illustrated in Figure 2.6. The frequency plot in Figure 2.4 corresponds to configuration P in Figure 2.8.

We note that the center of gravity G_Q in configuration Q is lower than G_P which means that the unsymmetric configuration Q is the stable one. It thus follows that when the pendulums are perturbed from configuration P they move to the stable configuration Q and oscillate about it. The plot of Figure 2.4 in the range $d < d_{CR}$ indicates that the system has moved from configuration P to Q and gives the initial exponential rate of deviation.

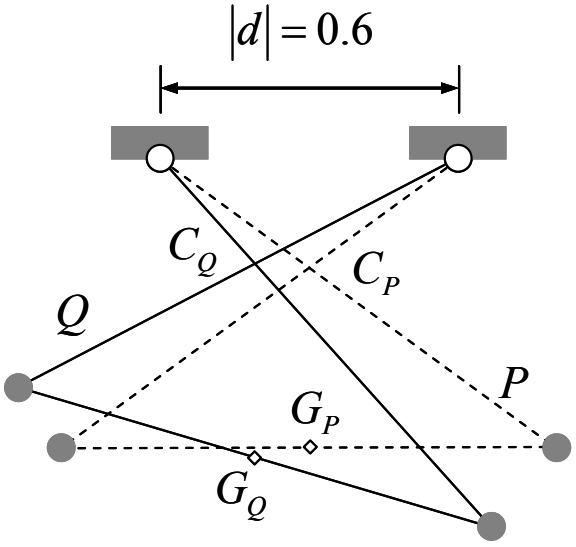

Figure 2.8 Contrary to intuition, configuration P is unstable, while Q is stable

In summary, when $d \geq d_{CR}$ the pendulum system is stable for each finite perturbation. But if the negative distance d is increased in absolute value sense beyond d_{CR} then the equilibrium configuration where Link 2 is horizontal is no longer stable. If d is slightly smaller than d_{CR} the effect of the instability is that the pendulums oscillate about a slightly perturbed unsymmetric configuration. Inspection of Figure 2.8 suggests that the instability in the system is substantial. A change in the distance between the pivots of $D - D_{CR} = -0.0126$ caused a shift of $16.6°$ in the static position of Link 2.

Table 2.1: Stable and unstable configurations for $d = -0.6$

	ϑ_1	ϑ_2	ϑ_3	λ	μ
Stable configuration Q	$-62.78°$	$73.40°$	$-138.00°$	1.2306	1.3669
Unstable configuration P	$-53.13°$	$90°$	$-126.86°$	1.3333	1.0000

Example 2.1

We wish to find the frequency of oscillation about the stable equilibrium when $d = -0.6$. The frequency plot in Figure 2.4 does not provide the answer to this problem. We substitute the data from Table 2.1, corresponding to the stable configuration Q, in $\mathbf{K}$ and $\mathbf{M}$ defined by equations (2.18)-(2.20). With these matrices, the eigenvalue problem (2.33) gives

$$\omega^2 = 0.0759 \frac{g}{l} \tag{2.42}$$

and the corresponding eigenvector is,

$$\mathbf{v} = \begin{pmatrix} -.4584 & -.8507 & -.6092 & -.6073 & 1 \end{pmatrix}^T \tag{2.43}$$

This relatively small natural frequency of oscillations is, from an engineering point of view, alarming. It indicates that the stable equilibrium Q is weak. In this example, as in general, the non-linear part of the problem of determining the stable equilibrium position is the dominant one in complexity.

2.6 Equations of Motion of the Discrete Model of a Catenary

In this section, we extend the double pendulum system model to higher dimensions by considering a catenary. To this end, consider a catenary of total length l and total mass M pinned by two horizontally leveled pegs, O_A and O_B, distance d apart, as in Figure 2.9. A chain of pendulum with n masses and $n+1$ inflexible weightless links presents a lumped parameter model for the catenary of dimension n. The length of each link in the model is $h = l/(n+1)$ and

the value of each mass is $m = M/n$. When the model is large enough, its few lowest natural frequencies approximate accurately the corresponding natural frequencies of the catenary.

2.6.1 Equations of Motion

The potential energy in the system is

$$V = mgh\sum_{k=1}^{n}(n+1-k)(\cos\vartheta_k - \cos\theta_k) \tag{2.44}$$

and the kinetic energy is

$$T = \frac{1}{2}mh^2\sum_{k=1}^{n}(n+1-k)\dot{\theta}_k^2 + mh^2\sum_{i=1}^{n-1}\sum_{j=i+1}^{n}(n+1-j)\dot{\theta}_i\dot{\theta}_j\cos(\theta_j - \theta_i). \tag{2.45}$$

The symmetric equations (2.16)-(2.20), governing small vibrations in the double pendulum system is highly structured. The stiffness matrix corresponding to the lumped parameter model of the catenary is

$$\mathbf{K} = g\begin{bmatrix} \kappa_{11} & 0 & 0 & \cdots & \cos\vartheta_1 & -\sin\vartheta_1 \\ 0 & \kappa_{22} & 0 & \cdots & \cos\vartheta_2 & -\sin\vartheta_2 \\ 0 & 0 & \kappa_{33} & \cdots & \cos\vartheta_3 & -\sin\vartheta_3 \\ \vdots & \vdots & \vdots & \ddots & \vdots & \vdots \\ \cos\vartheta_1 & \cos\vartheta_2 & \cos\vartheta_3 & \cdots & 0 & 0 \\ -\sin\vartheta_1 & -\sin\vartheta_2 & -\sin\vartheta_3 & \cdots & 0 & 0 \end{bmatrix}, \qquad \mathbf{K} \in \Re^{n+3\times n+3} \tag{2.46}$$

where

$$\kappa_{ii} = ((n+1-i)-\mu)\cos\vartheta_i - \lambda\sin\vartheta_i, \quad i = 1,2,...,n+1\ . \tag{2.47}$$

The mass matrix has the form

$$\mathbf{M} = \begin{bmatrix} \mathbf{M}_{11} & \mathbf{0} \\ \mathbf{0} & \mathbf{0} \end{bmatrix}, \qquad \mathbf{M} \in \Re^{n+3\times n+3}, \qquad \mathbf{M}_{11} \in \Re^{n\times n} \tag{2.48}$$

where

$$\mathbf{M}_{11} = h\begin{bmatrix} m_{11} & m_{12} & \cdots & m_{1n} \\ m_{21} & m_{22} & \cdots & m_{2n} \\ \vdots & \vdots & \vdots\vdots\vdots & \vdots \\ m_{n1} & m_{n2} & \cdots & m_{nn} \end{bmatrix} \tag{2.49}$$

and

$$m_{ij} = (n+1-\max\{i,j\})\cos(\vartheta_j - \vartheta_i), \qquad i = 1,2,...,n\,, \quad j = 1,2,...,n\,. \tag{2.50}$$

Example 2.2

This example demonstrates the development of the mass matrix corresponding to the lumped-parameter model of the catenary of order $n = 4$.

$$\mathbf{M}_{11} = h\begin{bmatrix} 4 & 3\cos(\vartheta_2-\vartheta_1) & 2\cos(\vartheta_3-\vartheta_1) & \cos(\vartheta_4-\vartheta_1) \\ 3\cos(\vartheta_1-\vartheta_2) & 3 & 2\cos(\vartheta_3-\vartheta_2) & \cos(\vartheta_4-\vartheta_2) \\ 2\cos(\vartheta_1-\vartheta_3) & 2\cos(\vartheta_2-\vartheta_3) & 2 & \cos(\vartheta_4-\vartheta_3) \\ \cos(\vartheta_1-\vartheta_4) & \cos(\vartheta_2-\vartheta_4) & \cos(\vartheta_3-\vartheta_4) & 1 \end{bmatrix}. \tag{2.51}$$

Note that $\mathbf{M}_{11}$ is symmetric for all model order n since $\cos(\vartheta_i - \vartheta_j) = \cos(\vartheta_j - \vartheta_i)$. ■

The static equilibrium data, ϑ_k, $k = 1,2,...,n+1$, λ and μ, used in evaluating $\mathbf{K}$ and $\mathbf{M}$ are obtained by the set of $n+3$ static equilibrium equations

$$\mathbf{f} = \begin{pmatrix} f_1 \\ f_2 \\ \vdots \\ f_{n+3} \end{pmatrix} = \begin{cases} ((n+1-k)-\mu)\sin\vartheta_k + \lambda\cos\vartheta_k = 0 & k = 1,2,...,n+1 \\ \sin\vartheta_1 + \sin\vartheta_2 + ...\sin\vartheta_{n+1} - d/h = 0 & k = n+2 \\ \cos\vartheta_1 + \cos\vartheta_2 + ...\cos\vartheta_{n+1} = 0 & k = n+3 \end{cases}, \tag{2.52}$$

the counterparts of (2.10). The solution of (2.52) defines the stiffness and mass matrices (2.46) through (2.50), which determine the natural frequencies of the system via the eigenvalue problem (2.33).

In general, the difficult part of the problem is that of solving the set of nonlinear equation (2.52). For a symmetric chain, it is possible to obtain a closed-form solution, as done in Irvine (1981) p. 102. For a non-symmetric chain, Newton's method for solving a set of nonlinear equations may be used. The initial guess for the angles ϑ_k could be taken from the slopes of the appropriate points in the analytical solution of the shape of the corresponding continuous catenary.

We will now show that the nonlinear system (2.52) may be solved by using a one-parameter iterative process. Adding f_1 and f_{n+1} gives

$$(n-\mu)\sin\vartheta_1 + \lambda\cos\vartheta_1 - \mu\sin\vartheta_{n+1} + \lambda\cos\vartheta_{n+1} = (n-2\mu)\sin\vartheta_1 = 0 \tag{2.53}$$

since by symmetry of the catenary $\vartheta_{n+1} = \pi - \vartheta_1$. For $d > 0$ the angle ϑ_1 does not vanish, and

hence

$$\mu = \frac{n}{2}. \tag{2.54}$$

It then follows from $f_{n+1} = 0$ that

$$\lambda = \frac{n}{2}\tan\vartheta_{n+1} = -\frac{n}{2}\tan\vartheta_1. \tag{2.55}$$

Substituting (2.54) and (2.55) in the general expression for f_k, $k = 1,2,...,n+1$, given in (2.52), yields

$$\vartheta_k = \tan^{-1}\frac{n\tan\vartheta_1}{n+2-2k}, \qquad k = 1,2,...,n+1 \tag{2.56}$$

Note that the solution obtained is symmetric in the sense that $\vartheta_{n+2-k} = \pi - \vartheta_k$. In particular, if n is odd the middle link is horizontal since

$$\vartheta_{n/2+1} = \lim_{\alpha\to\infty}\tan^{-1}\alpha = \pi/2. \tag{2.57}$$

It thus follows that (2.54)-(2.56) determine a stable static equilibrium of the catenary. By the symmetry of the angles noted above the vertical constraint $f_{n+3} = 0$ is satisfied inherently. The horizontal constraint $f_{n+2} = 0$ would not be generally satisfied, unless by chance.

We may thus choose ϑ_1 as an iterative parameter and obtain λ from (2.55). Then ϑ_k, $k = 2,3,...,n+1$ may be obtained by (2.56). All equations in (2.52) are then satisfied apart from the horizontal constraint, $f_{n+2} = 0$. The system of equations (2.52) may thus be solved by a shooting method where ϑ_1 is the iterative parameter and $f_{n+2} = 0$ is the control.

2.6.2 Results

For the sake of illustration, we consider a catenary of length $l = 3$ which is pinned at O_A and O_B, leveled horizontally distance $d = 2$ apart, as shown in Figure 2.9 . A Cartesian coordinate system is used to describe the shape $y(x)$ of the catenary.

The symmetric deflection of the catenary is

$$y(x) = C\cosh\frac{x}{C}, \tag{2.58}$$

where C is a constant. The value of C is determined by the requirement that the length of the catenary is l,

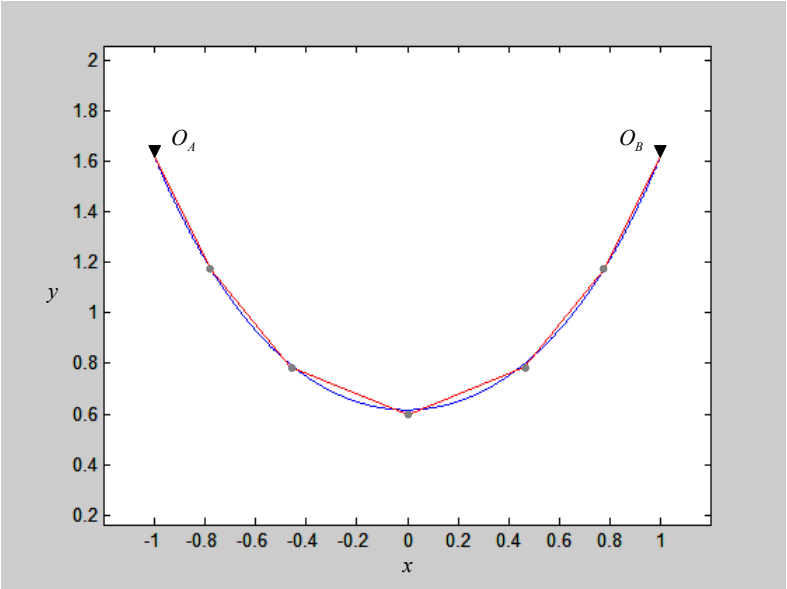

Figure 2.9 The catenary and its lumped parameter model of order $n = 5$

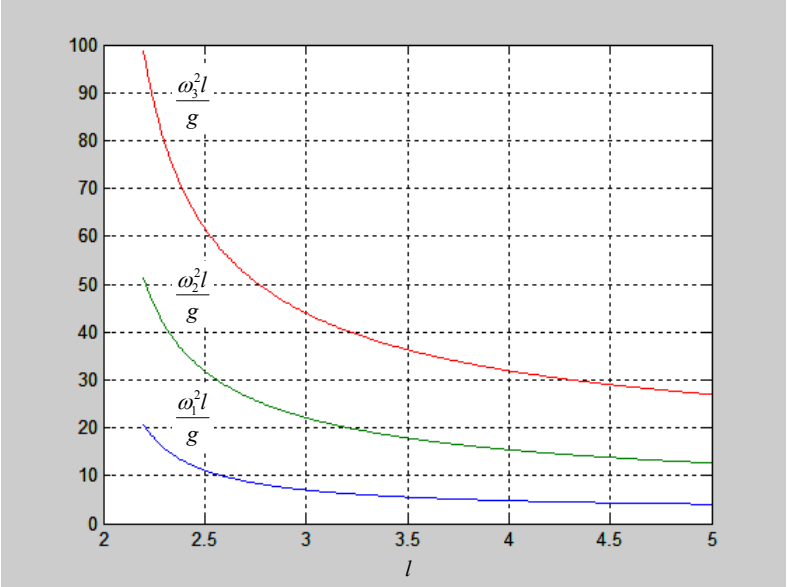

Figure 2.10 The first three natural frequencies of a symmetric catenary of length l pinned at distance $d = 2$ apart

$$\int_{O_A}^{O_B} ds = 2\int_0^1 \sqrt{1+y'^2}\,dx = 2\int_0^1 \cosh\frac{x}{C}dx = l, \tag{2.59}$$

where s is a curved coordinate that runs along the center line of the catenary and represents its arc length, prime denotes derivative with respect to x. It thus follows from (2.59) that

$$\sinh\frac{1}{C}=\frac{l}{2C}. \tag{2.60}$$

The first three natural frequencies of a symmetric catenary, which is hanged by pines at O_A and O_B, distance $d=2$ apart, as functions of its length, $2.2<l<5$, are shown in Figure 2.10.

2.6.3 Validation of the Results

One would expect the characterization of small oscillations of the catenary to be a classical result in Mechanics and Applied Mathematics. It appears that such a characterization is absent in the old classics such as Ziegler (1968) and Timoshenko (1961). We could not find it in modern books such as Irvine (1981) either. At this current state of the art, the archive journal literature in vibration is a vast ocean and relevant results could be easily missed. A search of the Web of Science exposed many papers dealing with modeling and analysis of more complex related problems. But we could not find a reference that gives a simple and direct validation of the results obtained in section 2.6.2. We, therefore, conduct here an asymptotic analysis that reduces the catenary to simpler systems.

The first reduction of the problem is when $d=0$. Examples 2.3 and 2.4 deal with this case for various values of n.

Example 2.3

If $l=2$, $d=0$ and $n=1$ then

$$\mathbf{M}=h\begin{bmatrix}1&0&0&0\\0&0&0&0\\0&0&0&0\\0&0&0&0\end{bmatrix},\qquad \mathbf{K}=g\begin{bmatrix}0.5&0&1&0\\0&0.5&-1&0\\1&-1&0&0\\0&0&0&0\end{bmatrix}. \tag{2.61}$$

The eigenvalue problem (2.33) has one eigenvalue

$$\omega^2=\frac{g}{h}. \tag{2.62}$$

The system vibrates like a simple pendulum of length $h=1$. ■

Remark 1: To avoid singularity in both $\mathbf{K}$ and $\mathbf{M}$, which hampers numerical computations, when $d=0$ the last row and column in both $\mathbf{K}$ and $\mathbf{M}$ could be omitted.

The case where $n = 2$ and $d = 0$ was addressed in Section 2.5.2. It was verified that the system vibrates in that case like the compound pendulum of Figure 2.5.

Example 2.4

If $l = 4$, $d = 0$ and $n = 3$, then with the last vanishing rows and column in $\mathbf{M}$ and $\mathbf{K}$ omitted, we have

$$\mathbf{M} = h\begin{bmatrix} 3 & 2 & -1 & 0 & 0 \\ 2 & 2 & -1 & 0 & 0 \\ -1 & -1 & 1 & 0 & 0 \\ 0 & 0 & 0 & 0 & 0 \\ 0 & 0 & 0 & 0 & 0 \end{bmatrix}, \qquad \mathbf{K} = g\begin{bmatrix} 1.5 & 0 & 0 & 0 & 1 \\ 0 & 0.5 & 0 & 0 & 1 \\ 0 & 0 & 0.5 & 0 & -1 \\ 0 & 0 & 0 & 1.5 & -1 \\ 1 & 1 & -1 & -1 & 0 \end{bmatrix}. \tag{2.63}$$

The eigenvalue problem (2.33) has three eigenvalues

$$\omega_1^2 = \frac{1}{2}\left(3 - \sqrt{3}\right)\frac{g}{h}, \qquad \omega_2^2 = \frac{2g}{h} \qquad \omega_3^2 = \frac{1}{2}\left(3 + \sqrt{3}\right)\frac{g}{h}. \tag{2.64}$$

The corresponding mode shapes are shown in Figure 2.11. Note that these mode shapes are symmetric about the vertical axis.

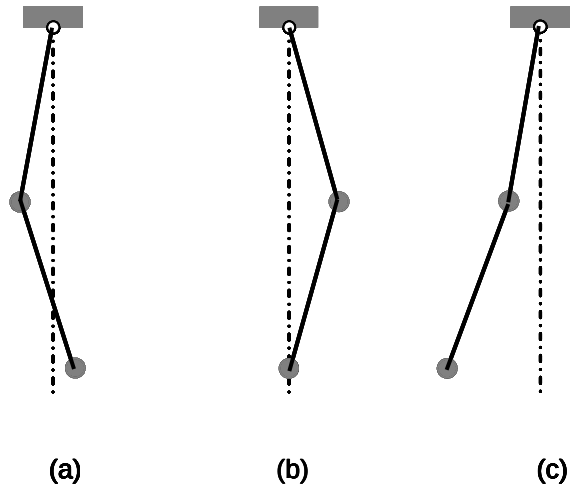

Figure 2.11 Mode shape for a pendulum chain, $n = 3$

Consider now a double pendulum of equal rods $h_1 = h_2 = h$ and unequal masses $m_1 = 2m_2 = 2m$. Its equations of motion for that system are

$$mh\begin{bmatrix} 3 & 1 \\ 1 & 1 \end{bmatrix}\begin{pmatrix} \ddot{\varphi}_1 \\ \ddot{\varphi}_2 \end{pmatrix} + mg\begin{bmatrix} 3 & 0 \\ 0 & 1 \end{bmatrix}\begin{pmatrix} \varphi_1 \\ \varphi_2 \end{pmatrix} = \begin{pmatrix} 0 \\ 0 \end{pmatrix}. \tag{2.65}$$

The first and the third frequency in (2.64) are natural frequencies of the pendulum (2.65). If the motion in (2.65) is restricted such that $\varphi_1 = -\varphi_2$ then the natural frequency of the constrained system is $2g/h$, the second frequency in (2.64).

The solution for the case $n = 3$ agrees well with the underlying physical rules. ■

2.7 Experiment

An experiment was conducted to verify the results of Section 2.5. Two small holes, at a distance $l = 305\,\text{mm}$ apart, were made in a steel bar with physical dimensions of $320 \times 18 \times 4\,\text{mm}^3$. Two loops of in-extensible strings of negligible mass, each of approximately effective length l, were inserted into the holes of the bar at one end and in small hooks that are mounted on a smooth board, at the other end, as shown in Figure 2.12.

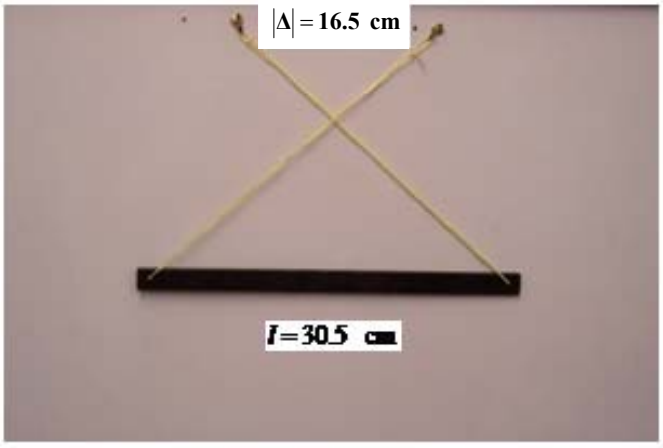

(a)

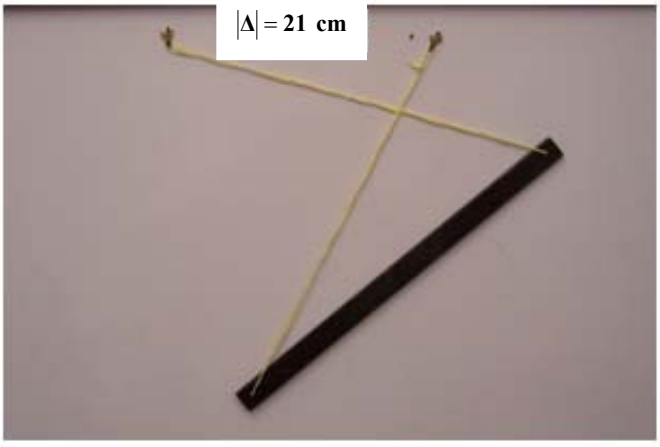

(b)

Figure 2.12 Experiments showing the (a) stable symmetric state and (b) stable asymmetric state

The board confines the steel bar to be in an in-plane configuration. Its smoothness was designed to reduce frictional effects that were not considered in the theoretical model. It might be argued that the *bar-string* system used in the experiment is different from the constrained double pendulum system that we have studied. However, the two systems are *statically equivalent* and their dynamics for small perturbations are related to each other by a scale factor. . Suppose that the mass of the steel bar is $M = 2m$ and that its moment of inertia about its center of gravity is I_G.

Then, when the bar-string system is perturbed from its equilibrium, its total potential energy is

$$V = 2mgh\,, \tag{2.66}$$

where h is the vertical elevation of the center of gravity. Equation (2.66) also describes the total potential energy of the constrained double pendulum system when it undergoes similar perturbation. In addition, the two systems have the same geometrical constraints, (2.5) and (2.6). Since the equations of equilibrium are determined by minimization of the potential energy subject to the constraints, we conclude that the equations of equilibrium for the two systems are the same. Consequently the two systems have the same static equilibrium configurations.

When the pendulum system is slightly perturbed its kinetic energy is

$$T_P = mv^2 + \frac{ml^2\dot{\theta}^2}{4} \tag{2.67}$$

where v is the linear velocity of the center of gravity for the pendulum system, i.e., the mid point of link 2, and $\dot{\theta}$ is the angular velocity of link 2. The quantity v is related to $\dot{\theta}$ by a scale factor due to the constraints. Let $v = \alpha\dot{\theta}$, where α is the proportionality constant having physical dimension of length. Then the kinetic energy for the pendulum system is

$$T_P = m\left(\alpha^2 + \frac{l^2}{4}\right)\dot{\theta}^2\,. \tag{2.68}$$

By a similar process the kinetic energy for the bar-string system is

$$T_B = m\left(\alpha^2 + \frac{I_G}{2m}\right)\dot{\theta}^2\,. \tag{2.69}$$

Since the dynamic equations are obtained by minimization of the *action*, $V - T$, subject to the constraints, and since $I_G < ml^2/2$, the pendulum system is slower than the bar-string system, but from all other aspects the two systems are identical dynamically. It is therefore expected that the bar-string and the double pendulum system have the same equilibrium and the same kind of equilibrium state.

When the distance between the pivots was $|\Delta| = 165\,\text{mm}$ the steel bar was approximately horizontal, as shown in Figure 2.12 (a). Small deviation from horizontal position is attributed to frictional effects and imperfections in the string's length and leveling of the pegs. This case corresponds to $|d| = 0.541 < |d_{CR}| = 0.587$. This result is in agreement with the theory.

When the distance was increased in negativity to $|\Delta| = 210\,\text{mm}$, the steel bar tilted at an angle of about $40°$ with the horizon and remained in an asymmetric equilibrium, as shown in Figure 2.12 (b). This case corresponds to $|d| = 0.688 > |d_{CR}| = 0.587$. The counterintuitive result predicted by the theory has thus been confirmed. The horizontal configuration of the bar is unstable.

2.8 Concluding Remarks

The constrained double pendulum system is a one-degree-of-freedom system. We could in principle, reduce the number of equations, from the five used, to one differential equation, by substitution of the variables of four of the equations in the remaining one. The gain would be a marginal increase in computational speed of the extraction of the eigenvalue. However, by adopting such a strategy, apart from the obvious added complexity involved in substitution, we would lose insight of the governing equations and the dynamics of the internal variables, i.e., the reactions of the supports $\hat{\lambda}$ and $\hat{\mu}$, and the oscillations of θ_2 and θ_3. Obviously, the simple extension of the results to a chain of pendulums of higher dimension, done in section 2.6, would become very much involved, if not impossible. That is why we adopted the methodology of using a large, revealing model that does not scramble the natural data.

Chapter 3
Stability Boundaries of a Mechanical Controlled System with Time Delay

The problem of determining the critical time delay where a class of state-feedback-controlled mechanical system may lose or gain stability in a closed-form manner is considered here. It is shown that for SIMO systems the problem may be reduced by using singular value decomposition to the problem of finding the roots of a certain polynomial. This technique cannot be extended to the MIMO controlled system. Two numerical methods are developed to solve this case. One method involves Newton's iterations and the other method involves bisection for multiple functions.

3.1 Motivation

State feedback control involves measuring the system states and feeding the signal into the processor following which the processor conditions the signals according to the control law. The resulting control signal is then fed into the actuators which apply the control on the system. We consider the case where there exists a time delay between the measurement of states and application of the control input to the system. Such a delay can occur in engineering applications where sensors and actuators are non-collocated or where the control signal is computed remotely and then wirelessly transmitted to the actuators (e.g., unmanned air, ground, and underwater vehicles).

The dynamics of a mechanical MIMO controlled system with time delay is governed by the set of second order differential equations,

$$\mathbf{M}\ddot{\mathbf{x}}(t)+\mathbf{C}\dot{\mathbf{x}}(t)+\mathbf{K}\mathbf{x}(t)=\mathbf{B}\mathbf{u}(t-\tau),\quad \mathbf{M},\mathbf{C},\mathbf{K}\in\Re^{n\times n},\quad \mathbf{B}\in\Re^{n\times m},\ \mathbf{u}\in\Re^{m},\quad m\le n, \tag{3.1}$$

where

$$\mathbf{u}(t-\tau)=\mathbf{F}^{T}\dot{\mathbf{x}}(t-\tau)+\mathbf{G}^{T}\mathbf{x}(t-\tau),\qquad \mathbf{F},\mathbf{G}\in\Re^{n\times m}. \tag{3.2}$$

The *mass* matrix $\mathbf{M}$ is symmetric positive definite and the *damping* and *stiffness* matrices, $\mathbf{C}$ and $\mathbf{K}$, are symmetric semi-positive definite matrices. The *control* vector $\mathbf{u}$ consists of the sum of the products of the control *gain* matrices $\mathbf{F}$, $\mathbf{G}$, and the *state* $\dot{\mathbf{x}}$, $\mathbf{x}$, respectively. The control force $\mathbf{Bu}$ is the product of the *input* matrix $\mathbf{B}$ and $\mathbf{u}$. The scalar *time delay* τ denotes the lag between the measurement of the state and the application of the corresponding control force. It is not difficult to show that (3.1) is equivalent to (1.1) and (1.2). The main results of this chapter pertain only to systems described by (3.1) and (3.2).

Separation of variables

$$\mathbf{x}(t)=\mathbf{v}e^{\lambda t} \tag{3.3}$$

applied to (3.1) and (3.2) yields the *transcendental eigenvalue problem*,

$$\mathbf{R}(\tau,\lambda)\mathbf{v} = \left(\lambda^2\mathbf{M} + \lambda\mathbf{C} + \mathbf{K} - e^{-\lambda\tau}\mathbf{B}\left(\lambda\mathbf{F}^T + \mathbf{G}^T\right)\right)\mathbf{v} = \mathbf{0}. \tag{3.4}$$

It is well known that depending on τ the system may be unstable. In this case at least one of the eigenvalues $\lambda \equiv \alpha + i\beta$, of (3.4) has positive real part, $\alpha > 0$. The chapter deals with the problem of finding the critical time delays that the system may *lose* or *gain* stability.

For the critical time delay τ, where the system is in transient from stable to unstable states or *vice versa*, the eigenvalues of (3.4) are purely imaginary. In principle the problem could be stated as finding λ and τ satisfying:

$$f_1(\tau,\lambda) = \det(\mathbf{R}(\tau,\lambda)) = 0, \quad f_2(\tau,\lambda) = \lambda\bar{\lambda} + \lambda^2 = 0, \quad f_3(\tau,\lambda) = \tau\bar{\tau} - \tau^2 = 0, \tag{3.5}$$

where bars denote complex conjugation. The second equation $f_2(\tau,\lambda)$ in (3.5) expresses the condition that λ is purely imaginary and the third equation, $f_3(\tau,\lambda)$, ensures that τ is real. The difficulty in solving the equations in (3.5) stems from the reality that $f_2(\tau,\lambda)$ and $f_3(\tau,\lambda)$ are generally not differentiable with respect to complex variables. As a result, iterative methods of solutions such as the Newton's method could not be employed.

Theorem 2

The poles of (3.4) are closed under conjugation. Equivalently we may say that the poles of (3.4) are *symmetric about the real axis* of the complex plane.

The characteristic polynomial associated with the *transcendental eigenvalue problem* (3.4) is a *Quasi-polynomial*. It is not obvious that the poles of a quasi-polynomial exhibit a similar behavior as is the case with a simple polynomial. We will now show that the poles of (3.4) appear in complex conjugate pairs.

Proof

Suppose that

$$s = \alpha + i\beta \qquad \mathbf{v} = \boldsymbol{\mu} + i\boldsymbol{\psi} \tag{3.6}$$

is a matrix pencil of (3.4). Substituting (3.6) in (3.4) gives

$$\left((\alpha+i\beta)^2\mathbf{M} + (\alpha+i\beta)\left(\mathbf{C} - e^{-(\alpha+i\beta)\tau}\mathbf{F}^T\right) + \mathbf{K} - e^{-(\alpha+i\beta)\tau}\mathbf{G}^T\right)(\boldsymbol{\mu} + i\boldsymbol{\psi}) = \mathbf{0} \tag{3.7}$$

Using Euler's formula for trigonometric and complex exponential functions

$$e^{i\theta} = \cos\theta + i\sin\theta$$

we obtain

$$\begin{aligned}&\left(\left(\alpha^2-\beta^2\right)\mathbf{M}+\alpha\,\mathbf{C}+\mathbf{K}-\alpha\,\mathbf{F}^T e^{-\alpha\tau}\cos\beta\tau-\beta\,\mathbf{F}e^{-\alpha\tau}\sin\beta\tau-\mathbf{G}^T e^{-\alpha\tau}\cos\beta\tau\right)(\boldsymbol{\mu})\\&\left(-2\alpha\beta\,\mathbf{M}-\beta\,\mathbf{C}-\alpha\,\mathbf{F}^T e^{-\alpha\tau}\sin\beta\tau+\beta\,\mathbf{F}e^{-\alpha\tau}\cos\beta\tau-\mathbf{G}^T e^{-\alpha\tau}\sin\beta\tau\right)(\boldsymbol{\psi})=\mathbf{0}\end{aligned}\tag{3.8}$$

and

$$\begin{aligned}&i\left(2\alpha\beta\,\mathbf{M}+\beta\,\mathbf{C}+\alpha\,\mathbf{F}^T e^{-\alpha\tau}\sin\beta\tau-\beta\,\mathbf{F}e^{-\alpha\tau}\cos\beta\tau+\mathbf{G}^T e^{-\alpha\tau}\sin\beta\tau\right)(\boldsymbol{\mu})\\&\left(\left(\alpha^2-\beta^2\right)\mathbf{M}+\alpha\,\mathbf{C}+\mathbf{K}-\left(\alpha\,\mathbf{F}^T e^{-\alpha\tau}+\mathbf{G}^T e^{-\alpha\tau}\right)\cos\beta\tau-\beta\,\mathbf{F}e^{-\alpha\tau}\sin\beta\tau\right)(i\boldsymbol{\psi})=\mathbf{0}\end{aligned}\tag{3.9}$$

since (3.8) and (3.9) are the real and imaginary parts of (3.4) respectively.

We will now show that,

$$\bar{s}=\alpha-i\beta\qquad\qquad\bar{\mathbf{v}}=\boldsymbol{\mu}-i\boldsymbol{\psi}\tag{3.10}$$

is a matrix pencil of (3.4) as well.

Substituting (3.10) in (3.4) gives

$$\left(\left(\alpha-i\beta\right)^2\mathbf{M}+\left(\alpha-i\beta\right)\left(\mathbf{C}-e^{-(\alpha-i\beta)\tau}\mathbf{F}^T\right)+\mathbf{K}-e^{-(\alpha-i\beta)\tau}\mathbf{G}^T\right)(\boldsymbol{\mu}-i\boldsymbol{\psi})=\mathbf{0}\tag{3.11}$$

Using Euler's formula for trigonometric and complex exponential functions and separating the real and imaginary parts, we get

$$\begin{aligned}&\left(\left(\alpha^2-\beta^2\right)\mathbf{M}+\alpha\,\mathbf{C}+\mathbf{K}-\alpha\,\mathbf{F}^T e^{-\alpha\tau}\cos\beta\tau-\beta\,\mathbf{F}e^{-\alpha\tau}\sin\beta\tau-\mathbf{G}^T e^{-\alpha\tau}\cos\beta\tau\right)(\boldsymbol{\mu})\\&\left(-2\alpha\beta\,\mathbf{M}-\beta\,\mathbf{C}-\alpha\,\mathbf{F}^T e^{-\alpha\tau}\sin\beta\tau+\beta\,\mathbf{F}e^{-\alpha\tau}\cos\beta\tau-\mathbf{G}^T e^{-\alpha\tau}\sin\beta\tau\right)(\boldsymbol{\psi})=\mathbf{0}\end{aligned}\tag{3.12}$$

and

$$\begin{aligned}&-i\left(2\alpha\beta\,\mathbf{M}-\beta\,\mathbf{C}-\alpha\,\mathbf{F}^T e^{-\alpha\tau}\sin\beta\tau+\beta\,\mathbf{F}e^{-\alpha\tau}\cos\beta\tau-\mathbf{G}^T e^{-\alpha\tau}\sin\beta\tau\right)(\boldsymbol{\mu})\\&\left(\left(\alpha^2-\beta^2\right)\mathbf{M}+\alpha\,\mathbf{C}+\mathbf{K}-\left(\alpha\,\mathbf{F}^T e^{-\alpha\tau}+\mathbf{G}^T e^{-\alpha\tau}\right)\cos\beta\tau-\beta\,\mathbf{F}e^{-\alpha\tau}\sin\beta\tau\right)(-i\boldsymbol{\psi})=\mathbf{0}\end{aligned}\tag{3.13}$$

by virtue of (3.8) and (3.9). It thus follows that if s is an eigenvalue of (3.4) so is $\bar{s}$, i.e., the eigenvalues are symmetric about the x axis.

Generally, when (3.1) includes all non-vanishing matrices with τ and the norms of $\mathbf{F}$ and $\mathbf{G}$ are sufficiently small, the system is stable for symmetric positive definite $\mathbf{M}$, $\mathbf{C}$ and $\mathbf{K}$. The stability boundary is determined by the condition that the real part of s vanishes. In this chapter, we will give a closed form solution for determining τ that makes $\mathrm{Re}(s)=0$ for the SIMO case where both $\mathbf{F}$ and $\mathbf{G}$ have unit rank. The general MIMO system is also analyzed and two methods are proposed to determine the stability boundary of the problem.

3.2 Literature Review

The early paper by Satche (1949) presented a graphical stability test based on an elegant extension of the Nyquist method, while the more recent papers have focused with the development of an analytic stability criteria. Thowsen (1982) proposed a necessary and sufficient condition for delay independent asymptotic stability of linear differential difference equations with retardation. The conditions are easily tested when the system order and the number of delays are not too high. Kamen (1980) studied the asymptotic stability of delay difference equations of the retarded type in terms of zero criteria for polynomials in two independent complex variables. It was observed that the asymptotic stability independent of delay can be expressed in terms of a (finitely) implementable algebraic criterion involving a two-variable polynomial.

Brierley et al. (1981) gave a new criterion for asymptotic stability of solutions of certain linear differential-difference equations (independent of the delay duration) is given in terms of solutions of a complex Lyapunov matrix equation. Mori (1985) derived several sufficient conditions which guarantee stability of linear time-delay systems. The results are expressed by succinct scalar inequalities and necessitate a certain tradeoff between sharpness and simplicity. A new stability criteria to characterize a bound for the delay time (how large the deviation of the delay time can be compared to the nominal zero value) of a linear time-delay system with or without uncertainties was presented by Su (1994). The criteria utilizes a matrix inequality with an optimization variable, such that less inequalities may be used and extra freedom is given to optimize the result, when the Razumikhin type theorem is applied to obtain the bound and the bound for the delay time. While it was shown that the optimization function is unimodal and line search algorithms should be applied to find the optimal value for the systems with no uncertainties, no analytical proof was provided.

Algorithms to check the asymptotic stability of delay independent systems were proposed by Su (1995). The algorithms obtained are computationally tractable since they only check the eigenvalues of two specially constructed matrices and some simple mathematical computations. Walton and Marshall (1987) gave a direct approach to the analysis of systems with single or commensurate delays. The finite polynomials arising in this direct method were shown to have useful sensitivity properties. Olgac and Jalili (1999) outlaid the use of multiple delayed resonators as a viable technique to suppress tonal oscillations completely at several locations on Multi-Degree of Freedom (MDOF) mechanical structures. The stability of the entire system was addressed utilizing a stability chart strategy. A *peeling-off* procedure was presented to simplify the stability assessment by converting the problem of multiple delayed resonators to a single delay representation. The agreement between stability charts and simulated time responses were shown by numerical examples.

Olgac and Sipahi (2002) presented a structural method for assessing the stability of linear time invariant systems with time delayed state feedback. The method involved a substitution for the exponential type transcendental terms in the characteristic equation to facilitate the determination of the root crossing points over the imaginary axis and the corresponding delays, following which the D-Subdivision method was deployed for the intervals of the delay, which renders the stability outlook of the system. It was concluded that time-delayed linear time-

invariant systems can have only finite number of purely imaginary characteristic roots and that these roots are generated by infinitely many discrete values of delays. The method solves all of these frequencies and the corresponding delays. Also, at each one of these finite number of imaginary roots, the root tendencies are invariant with respect to delay, i.e., increasing the delay causes the same root crossing direction. They move either to unstable or stable half plane at the given frequency regardless of the value of time delay which creates them.

Ram (2008) shed light on the fact that the problem of finding a parameter t and a repeated eigenvalue λ of a transcendental eigenvalue problem plays a crucial role in determining the stability of circulatory and gyroscopic continuous systems, such as buckling of columns by tangential forces and determining critical speeds in gyroscopic systems. It is remarkable that the problem of finding the critical time delay in mechanical controlled systems falls into this category.

3.3 Critical Time Delay in SIMO Controlled Systems

The SIMO controlled system is the case where $m = 1$. We denote

$$\mathbf{b} = \mathbf{B}, \quad \mathbf{f} = \mathbf{F}, \quad \mathbf{g} = \mathbf{G}, \quad u(t) = \mathbf{u}(t), \tag{3.14}$$

so that (3.1) and (3.2) take the form

$$\mathbf{M}\ddot{\mathbf{x}}(t) + \mathbf{C}\dot{\mathbf{x}}(t) + \mathbf{K}\mathbf{x}(t) = \mathbf{b}u(t-\tau), \tag{3.15}$$

and

$$u(t-\tau) = \mathbf{f}^T\dot{\mathbf{x}}(t-\tau) + \mathbf{g}^T\mathbf{x}(t-\tau). \tag{3.16}$$

applicable to the SIMO system. The corresponding transcendental eigenvalue problem is

$$\left(\lambda^2\mathbf{M} + \lambda\mathbf{C} + \mathbf{K} - e^{-\lambda\tau}\mathbf{b}\left(\lambda\mathbf{f}^T + \mathbf{g}^T\right)\right)\mathbf{v} = \mathbf{0}, \tag{3.17}$$

the counterpart of (3.4). We denote

$$\mathbf{y} = \begin{pmatrix} \mathbf{v} \\ \lambda\mathbf{v} \end{pmatrix}, \tag{3.18}$$

and write (3.17) in its first order realization form,

$$\left(\begin{bmatrix} \mathbf{0} & \mathbf{I} \\ -\mathbf{K} & -\mathbf{C} \end{bmatrix} - \lambda\begin{bmatrix} \mathbf{I} & \mathbf{0} \\ \mathbf{0} & \mathbf{M} \end{bmatrix} + e^{-\lambda\tau}\begin{bmatrix} \mathbf{0} & \mathbf{0} \\ \mathbf{b}\mathbf{g}^T & \mathbf{b}\mathbf{f}^T \end{bmatrix}\right)\begin{pmatrix} \mathbf{v} \\ \lambda\mathbf{v} \end{pmatrix} = \begin{pmatrix} \mathbf{0} \\ \mathbf{0} \end{pmatrix}, \tag{3.19}$$

or

$$\left(\mathbf{A} - \lambda\mathbf{B} + e^{-\lambda\tau}\mathbf{H}\right)\mathbf{y} = \mathbf{0}, \tag{3.20}$$

with the obvious definitions of $\mathbf{A}$, $\mathbf{B}$ and $\mathbf{H}$. Note that $\mathbf{H}$ is a rank-one matrix.

Equation (3.20) has a non-trivial solution $\mathbf{y} \neq \mathbf{0}$ if and only if the transcendental characteristic equation is singular,

$$\det\left(\mathbf{A} - \lambda\mathbf{B} + e^{-\lambda\tau}\mathbf{H}\right) = 0\,. \tag{3.21}$$

Let

$$\mathbf{H} = \mathbf{U}\boldsymbol{\Sigma}\mathbf{V}^T, \quad \boldsymbol{\Sigma} = diag\begin{pmatrix}\sigma & 0 & \cdots & 0\end{pmatrix} \tag{3.22}$$

be the singular value decomposition of the rank-one matrix $\mathbf{H}$.

Then (3.21) gives

$$\det\left(\mathbf{U}^T\left(\mathbf{A} - \lambda\mathbf{B}\right)\mathbf{V} + e^{-\lambda\tau}\boldsymbol{\Sigma}\right) = 0\,. \qquad . \tag{3.23}$$

We define

$$\mathbf{Q}(\lambda) \equiv \mathbf{U}^T\left(\mathbf{A} - \lambda\mathbf{B}\right)\mathbf{V}\,, \tag{3.24}$$

and find from (3.23) that

$$e^{-\lambda\tau} = -\frac{\det(\mathbf{Q})}{\sigma\det(\mathbf{Q}_1)} \equiv -P(\lambda)\,, \tag{3.25}$$

where $\mathbf{Q}_1(\lambda)$ is the leading principal submatrix of $\mathbf{Q}(\lambda)$. Note that $P(\lambda)$ is a rational polynomial,

$$P(\lambda) \equiv -\frac{N(\lambda)}{D(\lambda)}, \tag{3.26}$$

where

$$N(\lambda) = \det(\mathbf{Q}), \qquad D(\lambda) = \sigma\det(\mathbf{Q}_1)\,. \tag{3.27}$$

It follows from (3.25) that

$$\ln\left(e^{-\lambda\tau}\right) = -\lambda\tau = \ln\left(-P(\lambda)\right). \tag{3.28}$$

For any complex variable s we have

$$\ln s = \ln|s| + i\left(\arg s + 2\pi k\right), \qquad k = 0,1,2,\ldots. \tag{3.29}$$

Since $-\lambda\tau$ is purely imaginary (3.28) and (3.29) give

$$P(\lambda)\overline{P}(\lambda)=1. \tag{3.30}$$

Equation (3.31) may be written in the form

$$\frac{N(\lambda)\overline{D}(\lambda)\overline{N(\lambda)\overline{D}(\lambda)}}{\left(D(\lambda)\overline{D}(\lambda)\right)^2}=\frac{N(\lambda)\overline{N}(\lambda)}{D(\lambda)\overline{D}(\lambda)}=1, \tag{3.31}$$

or

$$N(\lambda)\overline{N}(\lambda)-D(\lambda)\overline{D}(\lambda)=0. \tag{3.32}$$

In general the polynomials $\overline{N}(\lambda)$ and $\overline{D}(\lambda)$ are not simply expressible in terms of the coefficients of $N(\lambda)$ and $D(\lambda)$. To circumvent this difficulty we define $N(\lambda)$ and $D(\lambda)$ by their coefficients

$$N(\lambda)=n_{2n}\lambda^{2n}+n_{2n-1}\lambda^{2n-1}+...+n_2\lambda^2+n_1\lambda+n_0, \tag{3.33}$$

$$D(\lambda)=d_{2n-1}\lambda^{2n-1}+d_{2n-2}\lambda^{2n-2}+d_{2n-3}\lambda^{2n-3}+...+d_2\lambda^2+d_1\lambda+d_0. \tag{3.34}$$

and denote

$$\hat{N}(\lambda)\equiv n_{2n}\lambda^{2n}-n_{2n-1}\lambda^{2n-1}+...+n_2\lambda^2-n_1\lambda+n_0, \tag{3.35}$$

$$\hat{D}(\lambda)\equiv -d_{2n-1}\lambda^{2n-1}+d_{2n-2}\lambda^{2n-2}-d_{2n-3}\lambda^{2n-3}+...+d_2\lambda^2-d_1\lambda+d_0. \tag{3.36}$$

Then, when λ is imaginary, we have

$$\hat{N}(\lambda)=\overline{N}(\lambda), \qquad \hat{D}(\lambda)=\overline{D}(\lambda). \tag{3.37}$$

It thus follows that equation (3.32) and

$$R(\lambda)\equiv N(\lambda)\hat{N}(\lambda)-D(\lambda)\hat{D}(\lambda)=0, \tag{3.38}$$

have common imaginary roots. We may thus find the roots of $R(\lambda)$. Each imaginary root λ_k of $R(\lambda)$ determine critical delays τ_{kr} via

$$\tau_{kr}=\frac{-\left(\arg\left(-P(\lambda_k)\right)+2\pi r\right)i}{\lambda_k}, \qquad r=...-1,0,1... \tag{3.39}$$

by virtue of (3.29).

Example 3.1

We demonstrate through this example the above development for the case of a 2-DOF SIMO system.

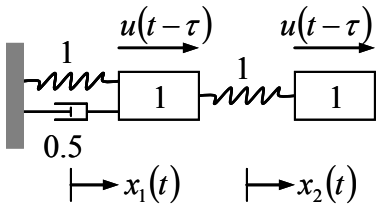

Figure 3.1 The two-degree-of-freedom system for Examples 3.1, 3.3 and 3.4

The dynamics of the system shown in Figure 3.1 is governed by the system of differential equations (3.15)-(3.16), where

$$\mathbf{M}=\begin{bmatrix}1 & 0\\ 0 & 1\end{bmatrix},\ \mathbf{C}=\begin{bmatrix}0.5 & 0\\ 0 & 0\end{bmatrix},\ \mathbf{K}=\begin{bmatrix}2 & -1\\ -1 & 1\end{bmatrix},\ \mathbf{b}=\begin{pmatrix}1\\ 1\end{pmatrix},\ \mathbf{f}=\begin{pmatrix}1\\ -2\end{pmatrix},\ \mathbf{g}=\begin{pmatrix}-1\\ -3\end{pmatrix}.$$

With first order realization (3.19) we have

$$\mathbf{A}=\begin{bmatrix}0 & 0 & 1 & 0\\ 0 & 0 & 0 & 1\\ -2 & 1 & -0.5 & 0\\ 1 & -1 & 0 & 0\end{bmatrix},\quad \mathbf{B}=\mathbf{I},\quad \mathbf{H}=\begin{bmatrix}0 & 0 & 0 & 0\\ 0 & 0 & 0 & 0\\ -1 & -3 & 1 & -2\\ -1 & -3 & 1 & -2\end{bmatrix}$$

$$\mathbf{U}=\frac{1}{\sqrt{2}}\begin{bmatrix}0 & -\sqrt{2} & 0 & 0\\ 0 & 0 & \sqrt{2} & 0\\ 1 & 0 & 0 & 1\\ 1 & 0 & 0 & 1\end{bmatrix}\quad \mathbf{\Sigma}=diag\begin{pmatrix}\sigma=\sqrt{30} & 0 & 0 & 0\end{pmatrix}$$

$$\mathbf{V}=\frac{1}{\sqrt{210}}\begin{bmatrix}-\sqrt{14} & -11 & -5\sqrt{3} & 0\\ -\sqrt{126} & -3 & 5\sqrt{3} & 0\\ \sqrt{14} & -4 & 2\sqrt{3} & -\sqrt{168}\\ -2\sqrt{14} & 8 & -4\sqrt{3} & -\sqrt{42}\end{bmatrix}.$$

It thus follows from (3.24) that

$$\mathbf{Q} = \frac{1}{\sqrt{840}}\left(\begin{bmatrix} \sqrt{7} & 13\sqrt{2} & 4\sqrt{6} & -2\sqrt{21} \\ -2\sqrt{14} & 8 & -4\sqrt{3} & -4\sqrt{42} \\ -4\sqrt{14} & 16 & -8\sqrt{3} & 2\sqrt{42} \\ 7\sqrt{7} & -29\sqrt{2} & -24\sqrt{6} & 2\sqrt{21} \end{bmatrix} - \lambda \begin{bmatrix} -2\sqrt{7} & 4\sqrt{2} & -2\sqrt{6} & 6\sqrt{21} \\ 2\sqrt{14} & 22 & 10\sqrt{3} & 0 \\ -6\sqrt{14} & -6 & 10\sqrt{3} & 0 \\ -6\sqrt{7} & 12\sqrt{2} & -6\sqrt{6} & -2\sqrt{21} \end{bmatrix}\right)$$

Equation (3.26) gives

$$P(\lambda) \equiv -\frac{N(\lambda)}{D(\lambda)} = -\frac{\lambda^4 + 0.5\lambda^3 + 3\lambda^2 + 0.5\lambda + 1}{\lambda^3 + 5\lambda^2 + 5.5\lambda + 11}.$$

Equations (3.35) and (3.36) give

$$\hat{N}(\lambda) = \lambda^4 - 0.5\lambda^3 + 3\lambda^2 - 0.5\lambda + 1, \qquad \hat{D}(\lambda) = -\lambda^3 + 5\lambda^2 - 5.5\lambda + 11.$$

From equation (3.38) we have

$$R(\lambda) = \lambda^8 + 6.75\lambda^6 - 3.5\lambda^4 - 74\lambda^2 - 120 = 0,$$

which has the purely imaginary roots

$$\lambda_{1,2} = \pm 2.3985\, i.$$

By (3.39), the critical time delay is

$$\tau = 0.1503 + \frac{2\pi r i}{\lambda}, \qquad r = ...,-1,0,1,...$$

3.4 Numerical Implementation of the Algorithm for SIMO Systems

For the algorithm developed in Section 3.3 to be implemented, it is required to evaluate the coefficients of the rational polynomial $P(\lambda)$ in (3.26), i.e., the coefficients of $N(\lambda)$ and $D(\lambda)$. In Example 3.1, $P(\lambda)$ was developed symbolically by expanding the determinants of $\mathbf{Q}(\lambda)$ and its leading principal submatrix $\mathbf{Q}_1(\lambda)$ using the analytical definition. Such an approach is not practical when dealing with systems of modest dimensions. We will now advise a procedure that allows determination of these coefficients numerically.

It follows from (3.27) and (3.24) that

$$N(\lambda) = \frac{\det\left(\mathbf{U}^T\mathbf{A}\mathbf{V}\right)\prod_{k=1}^{2n}(\lambda - \mu_k)}{\prod_{k=1}^{2n}\mu_k}, \tag{3.40}$$

where μ_k are the roots of $\det\mathbf{Q}(\lambda) = 0$. Similarly, we have

$$D(\lambda) = -\frac{\sigma\det\boldsymbol{\Psi}\prod_{k=1}^{2n-1}(\lambda - \rho_k)}{\prod_{k=1}^{2n-1}\rho_k} \tag{3.41}$$

where ρ_k are the roots of $\det\mathbf{Q}_1(\lambda) = 0$ and $\boldsymbol{\Psi}$ is the leading principal submatrix of $\mathbf{U}^T\mathbf{A}\mathbf{V}$.

The conjugates $\overline{N}$ and $\overline{D}$ may be conveniently expressed in λ for purely imaginary λ as follows

$$\overline{N}(\lambda) = \frac{\det\left(\mathbf{U}^T\mathbf{A}\mathbf{V}\right)\prod_{k=1}^{2n}(\lambda + \mu_k)}{\prod_{k=1}^{2n}\mu_k} \tag{3.42}$$

$$\overline{D}(\lambda) = \frac{\sigma\det\boldsymbol{\Psi}\prod_{k=1}^{2n-1}(\lambda + \rho_k)}{\prod_{k=1}^{2n-1}\rho_k} \tag{3.43}$$

Example 3.2

We illustrate the use of the algorithm developed above with the 5-DOF system shown in Figure 3.2.

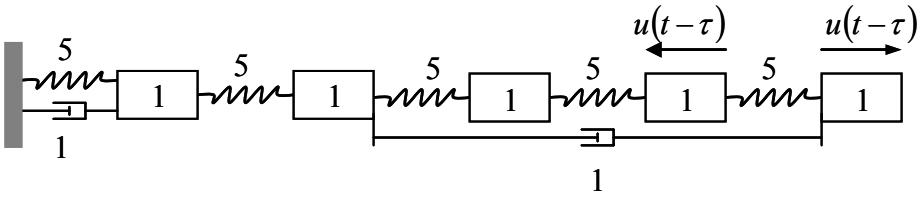

Figure 3.2 The five degrees of freedom system for Examples 3.2, 3.6 and 3.7

The dynamics of the system is governed by (3.15) and (3.16) with

$$\mathbf{M} = 5\mathbf{I}, \qquad \mathbf{C} = \begin{bmatrix} 1 & 0 & 0 & 0 & 0 \\ 0 & 1 & 0 & 0 & -1 \\ 0 & 0 & 0 & 0 & 0 \\ 0 & 0 & 0 & 0 & 0 \\ 0 & -1 & 0 & 0 & 1 \end{bmatrix}, \qquad \mathbf{K} = \begin{bmatrix} 10 & -5 & & & \\ -5 & 10 & -5 & & \\ & -5 & 10 & -5 & \\ & & -5 & 10 & -5 \\ & & & -5 & 5 \end{bmatrix},$$

$$\mathbf{b} = \begin{pmatrix} 0 \\ 0 \\ 0 \\ -1 \\ 1 \end{pmatrix}, \qquad \mathbf{f} = \begin{pmatrix} -1 \\ 0 \\ 1 \\ 0 \\ -1 \end{pmatrix}, \qquad \mathbf{g} = \begin{pmatrix} -1 \\ 0 \\ 0 \\ 0 \\ 1 \end{pmatrix}.$$

Table 3.1 Polynomial's coefficients, $r_{2k-1} = 0$, $k = 1,2,...,10$

k	n_k	d_k		k	r_k
0	-3125	625		0	9375000
1	-2500	-500		2	53531250
2	-9750	1125		4	99453125
3	-5125	-1300		6	67489375
4	-4775	-110		8	25205275
5	-1300	-450		10	5601270
6	-755	-29		12	758264
7	-110	-39		14	62983
8	-47	-1		16	3136
9	-3	-1		18	86
10	-1			20	1

By using (3.40) and (3.41) we obtained the polynomials $N(\lambda)$, $D(\lambda)$ and $R(\lambda)$. Their coefficients are listed in Table 3.1.

There are four purely imaginary roots to $R(\lambda) = 0$,

$$\lambda_{1,2} = \pm 2.4961i, \qquad \lambda_{3,4} = \pm 3.9677i,$$

with corresponding smallest positive time delays

$$\tau_{11} = 1.7135, \qquad \tau_{31} = 0.0120,$$

obtained by (3.39). The system is unstable at the smallest positive time delay, which in this case is given by τ_{31}.

3.5 Critical Time Delay in MIMO Controlled Systems

As stated in Section 3.1, the critical time delays are the real values of τ, in conjunction with purely imaginary λ, that render $\det(\mathbf{R}(\tau,\lambda))=0$. For the reason mentioned in Section 3.1, the straightforward approach of expressing the constraints on λ and τ via $f_2=f_3=0$ defined in (3.5) is not employable. To overcome this difficulty, we separate the complex equations in (3.4) into their real and imaginary components, and transfer the problem of determining the critical time delay into the following framework:

Problem 1

Given: $\mathbf{P}(\tau,\lambda)$
Find: real τ and purely imaginary λ such that λ is a repeated eigenvalue of

$$\mathbf{P}(\tau,\lambda)\mathbf{z}=\mathbf{0}, \tag{3.44}$$

with multiplicity $p>1$.

In Section 3.6, we address the numerical implementation of the algorithm developed in this section for the MIMO control system.

Since the Jacobian matrix associated with (3.5) is singular in the neighborhood of the solutions, the convergence of the Newton's method is linear. In Section 3.7 we develop a bisection algorithm for solving the problem. The problem involves multiple functions and bisection for trapping a solution that is developed for this case.

The transcendental eigenvalue problem for MIMO system is given by (3.4),

$$\mathbf{R}(\tau,\lambda)\mathbf{v}=\left(\lambda^2\mathbf{M}+\lambda\mathbf{C}+\mathbf{K}-e^{-\lambda\tau}\mathbf{B}\left(\lambda\mathbf{F}^T+\mathbf{G}^T\right)\right)\mathbf{v}=\mathbf{0}. \tag{3.45}$$

Since

$$\mathbf{H}=\mathbf{B}\left(\lambda\mathbf{F}^T+\mathbf{G}^T\right) \tag{3.46}$$

has $m>1$ singular values. It is generally not possible to write the determinant of $\mathbf{R}(\tau,\lambda)$ to express $e^{-\lambda\tau}$ in terms of a rational polynomial in λ, as done in (3.26). Consequently a closed form characterization of all critical time delays is not possible in this case.

In this section we develop a numerical method for finding the critical time delay for MIMO controlled systems.

We define

$$\lambda\equiv\alpha+i\beta, \quad \mathbf{v}=\boldsymbol{\psi}+i\boldsymbol{\rho}, \tag{3.47}$$

where α, β, τ, $\boldsymbol{\psi}$ and $\boldsymbol{\rho}$ are all real. Since λ is purely imaginary, $\alpha = 0$ and (3.45) may be written in the form

$$\left(-\beta^2\mathbf{M} + i\beta\mathbf{C} + \mathbf{K} - \left(\cos(\beta\tau) - i\sin(\beta\tau)\right)\mathbf{B}\left(i\beta\mathbf{F}^T + \mathbf{G}^T\right)\right)\left(\boldsymbol{\psi} + i\boldsymbol{\rho}\right) = \mathbf{0}. \tag{3.48}$$

The conditions that real and imaginary parts of equation (3.48) vanish simultaneously may be expressed as follows

$$\mathbf{P}(\beta,\tau)\mathbf{z} = \mathbf{0}, \tag{3.49}$$

where

$$\mathbf{P}(\beta,\tau) = \begin{bmatrix} \mathbf{P}_1 & \mathbf{P}_2 \\ -\mathbf{P}_2 & \mathbf{P}_1 \end{bmatrix}, \tag{3.50}$$

$$\mathbf{P}_1(\beta,\tau) = -\beta^2\mathbf{M} + \mathbf{K} - \cos(\beta\tau)\mathbf{B}\mathbf{G}^T - \beta\sin(\beta\tau)\mathbf{B}\mathbf{F}^T, \tag{3.51}$$

$$\mathbf{P}_2(\beta,\tau) = -\beta\mathbf{C} + \cos(\beta\tau)\beta\mathbf{B}\mathbf{F}^T - \sin(\beta\tau)\mathbf{B}\mathbf{G}^T, \tag{3.52}$$

and

$$\mathbf{z} = \begin{pmatrix} \boldsymbol{\psi} \\ \boldsymbol{\rho} \end{pmatrix}. \tag{3.53}$$

Lemma 3.1
For any real τ the eigenvalue s in $\mathbf{P}(s,\tau)$ has the double-symmetry property, i.e., if s is an eigenvalue of $\mathbf{P}(s,\tau)$ then $\bar{s}$ and $-s$ are also eigenvalues of $\mathbf{P}(s,\tau)$.

Proof

By (3.51) and (3.52)

$$\mathbf{P}_1(s,\tau) = \mathbf{P}_1(-s,\tau) \qquad \mathbf{P}_2(s,\tau) = -\mathbf{P}_2(-s,\tau), \tag{3.54}$$

since for each complex variable z, $\sin(z) = -\sin(-z)$ and $\cos(z) = \cos(-z)$. Since

$$\begin{bmatrix} \mathbf{P}_1 & -\mathbf{P}_2 \\ \mathbf{P}_2 & \mathbf{P}_1 \end{bmatrix} = \begin{bmatrix} \mathbf{I} & \mathbf{0} \\ \mathbf{0} & -\mathbf{I} \end{bmatrix}\begin{bmatrix} \mathbf{P}_1 & \mathbf{P}_2 \\ -\mathbf{P}_2 & \mathbf{P}_1 \end{bmatrix}\begin{bmatrix} \mathbf{I} & \mathbf{0} \\ \mathbf{0} & -\mathbf{I} \end{bmatrix} \tag{3.55}$$

the matrix $\mathbf{P}(s,\tau)$ and $\mathbf{P}(-s,\tau)$ are similarly congruent and share common eigenvalues.

For real τ we may in principle express $\cos(\varpi)$ and $\sin(\varpi)$ in $\mathbf{P}(s,\tau)$ by their Taylor series expansions and obtain a polynomial characteristic equation in s with real coefficients. Hence, the eigenvalues are closed under conjugation. □

Remark
For non-real τ the eigenvalues of $\mathbf{P}(s,\tau)$ are symmetric about the imaginary axis but not about the real axis.

Lemma 3.2
Each real eigenvalue β of $\mathbf{P}(\beta,\tau)$, associated with real τ, is a repeated eigenvalue with multiplicity $p>1$.

Proof

The proof of the lemma follows from the double-symmetry property of β established in Lemma 3.1. □

At this juncture, we may employ the method developed by Ram (2008) on finding the repeated roots in transcendental eigenvalue problems to determine the values of τ and its associated repeated eigenvalue β of the transcendental eigenvalue problem (3.45). For the sake of self sufficiency the method is described next.

We define

$$\phi(\beta,\tau)=\det(\mathbf{P})=0\,,\qquad \chi(\beta,\tau)=\frac{\partial\phi}{\partial\beta}=0\,, \tag{3.56}$$

and solve the two equations in (3.56) for the two unknowns β and τ by Newton's method as follows. We start with an initial guess for β and τ. Then we obtain the corrections δ_β and δ_τ to β and τ, respectively, via

$$\begin{pmatrix}\delta_\beta\\ \delta_\tau\end{pmatrix}=-\mathbf{J}\begin{pmatrix}\beta\\ \tau\end{pmatrix} \tag{3.57}$$

where $\mathbf{J}$ is the Jacobian matrix of partial derivatives,

$$\mathbf{J}=\begin{bmatrix}\partial\phi/\partial\beta & \partial\phi/\partial\tau\\ \partial\chi/\partial\beta & \partial\chi/\partial\tau\end{bmatrix}=\begin{bmatrix}\chi & \partial\phi/\partial\tau\\ \partial^2\phi/\partial\beta^2 & \partial\chi/\partial\tau\end{bmatrix}. \tag{3.58}$$

The process of obtaining corrections via (3.57) to the updated values of β and τ is repeated iteratively until the norm of $\begin{pmatrix}\delta_\beta & \delta_\tau\end{pmatrix}^T$ is sufficiently small.

We note that while by our definition α, β, τ, $\boldsymbol{\psi}$ and $\boldsymbol{\rho}$ are real, the eigenvalue problem (3.45) does not assure this characteristic. If however we start with an initial guess of β and τ, the corrections obtained by (the real) equation (3.57) are real at all stage. As a result, the Newton's method described is confined to determine the solutions along the real axis only. In this way, the difficulty of finding non-physical solutions of complex β and τ is circumvented.

The ideas described above are demonstrated by the following examples.

Example 3.3

By applying the Newton's method described, with tolerance of convergence $\varepsilon = 1e-14$ with respect to $\left\| \begin{pmatrix} \delta_\beta & \delta_\tau \end{pmatrix}^T \right\|$, we determined a critical time delay and its associated eigenvalue for the system in Example 1. Starting with initial guess $\beta = \tau = 2$ we obtained after 33 iterations

$$\beta = 2.3985 \qquad \tau = 10.6290 .$$

This solution corresponds to

$$\lambda = 2.3985i \qquad \tau = 0.1503 + \frac{2\pi r i}{\lambda}, \quad r = 4,$$

as in Example 3.1.

The relatively large number of iterations required to determine the solution indicates that the rate of convergence of the Newton's method is not quadratic. Indeed, the Jacobian matrix in the last iteration is

$$\mathbf{J} = \begin{bmatrix} -1.8190e-011 & -4.2788e-006 \\ 6.7815e+004 & 1.5633e+004 \end{bmatrix}$$

hinting to the possibility that $\partial\phi/\partial\tau = 0$ and consequently that the Jacobian matrix is singular at the point of solution. This issue will be further explored in this section. □

Example 3.4

We repeat Example 3.3 but now starting with a non-real initial guess, $\beta = 2 + i$, $\tau = 2$. After eleven iterations the program converged to the non-real solution

$$\beta = 1.7690 + 0.3529i \qquad \tau = 3.0080 - 0.7355i$$

which has no physical consequence.

Here β and τ obtained are not far away from the initial guess and the number of iterations, 11, is not high. For the last iteration the Jacobian matrix is

$$\mathbf{J} = \begin{bmatrix} 6.2528e-013 & -1.1369e-013i & 69.7411 & -9.1812i \\ 2.5470e+002 & -9.5789e+002i & 3.5131e+002 & -2.0607e+002i \end{bmatrix}$$

indicating Jacobian's regularity in the neighborhood of the solution, and in particular that generally $\partial\phi/\partial\tau \neq 0$ when complex arithmetic is done. □

The following Lemmas give an explanation to the linear convergence phenomenon hinted in Example 3.3.

Lemma 3.3
For any real s the root τ of $\phi(s,\tau)=0$ appears in complex conjugate pairs.

Proof

When s is real we may in principle express $\cos(\varpi s)$ and $\sin(\varpi s)$ in $\mathbf{P}(s,\tau)$ by their Taylor series expansions and obtain a polynomial in τ with real coefficients. Hence, if for real s, the parameter τ is a root of $\phi(s,\tau)=0$ so is $\bar{\tau}$. □

Lemma 3.4
The real solution s_k, τ_k of $\phi(s,\tau)=0$ is two-fold,

$$\phi(s_k,\tau_k) = \frac{\partial\phi(s_k,\tau_k)}{\partial s} = \frac{\partial\phi(s_k,\tau_k)}{\partial\tau} = 0.$$

Proof

The proof is a direct consequence of the complex conjugate closure of s and τ in the neighborhood of a real solution, established in Lemmas 3.1 and 3.3 □

3.6 Numerical Implementation of the Algorithm for MIMO Systems

In order to employ the algorithm for detecting the double eigenvalue of (3.49), it is required that the determinant of $\mathbf{P}(\beta,\tau)$ and its derivative be differentiated with respect to β and τ. A numerically-viable method for obtaining the derivatives of the determinant of a matrix is now given.

Let $\mathbf{L}(\xi)$ be a matrix of dimension $n\times n$. Let $\mathbf{L}_k(\xi)$ be the matrix $\mathbf{L}(\xi)$ with its *k*-th column replaced by its derivative with respect to ξ. Let $\mathbf{L}_{kr}(\xi)$ be the matrix $\mathbf{L}(\xi)$ with its *k*-th and *r*-th columns replaced by their derivatives with respect to ξ, respectively. The matrix $\mathbf{L}_{kk}(\xi)$ is $\mathbf{L}(\xi)$ with its *k*-th column replaced by its second derivative with respect to ξ.

Then,

$$\frac{d|\mathbf{L}|}{d\xi} = \sum_{k=1}^{n} |\mathbf{L}_k| \tag{3.59}$$

and

$$\frac{d^2|\mathbf{L}|}{d\xi^2} = \sum_{k=1}^{n} |\mathbf{L}_{kk}| + 2\sum_{k=1}^{n-1} \sum_{r=k+1}^{n} |\mathbf{L}_{kr}| . \tag{3.60}$$

Example 3.5

Suppose that

$$\mathbf{L} = \begin{bmatrix} \xi^3 & 2\xi \\ 3\xi & 4\xi^2 \end{bmatrix},$$

then

$$|\mathbf{L}| = 4\xi^5 - 6\xi^2 .$$

From the definitions above,

$$\mathbf{L}_1 = \begin{bmatrix} 3\xi^2 & 2\xi \\ 3 & 4\xi^2 \end{bmatrix}, \qquad \mathbf{L}_2 = \begin{bmatrix} \xi^3 & 2 \\ 3\xi & 8\xi \end{bmatrix},$$

and

$$\mathbf{L}_{11} = \begin{bmatrix} 6\xi & 2\xi \\ 0 & 4\xi^2 \end{bmatrix}, \qquad \mathbf{L}_{12} = \begin{bmatrix} 3\xi^2 & 2 \\ 3 & 8\xi \end{bmatrix}, \qquad \mathbf{L}_{22} = \begin{bmatrix} \xi^3 & 0 \\ 3\xi & 8 \end{bmatrix}.$$

It thus follows from (3.59) and (3.60) that

$$\begin{aligned} \frac{d|\mathbf{L}|}{d\xi} &= |\mathbf{L}_1| + |\mathbf{L}_2| \\ &= \begin{vmatrix} 3\xi^2 & 2\xi \\ 3 & 4\xi^2 \end{vmatrix} + \begin{vmatrix} \xi^3 & 2 \\ 3\xi & 8\xi \end{vmatrix} = 20\xi^4 - 12\xi \end{aligned}$$

and

$$\frac{d^2|\mathrm{L}|}{d\xi^2} = |\mathrm{L}_{11}| + 2|\mathrm{L}_{12}| + |\mathrm{L}_{22}|$$

$$= \begin{vmatrix} 6\xi & 2\xi \\ 0 & 4\xi^2 \end{vmatrix} + 2\begin{vmatrix} 3\xi^2 & 2 \\ 3 & 8\xi \end{vmatrix} + \begin{vmatrix} \xi^3 & 0 \\ 3\xi & 8 \end{vmatrix} = 80\xi^3 - 12.$$

Example 3.6

We use the system of Example 3.2 with the following MIMO control matrices

$$\mathbf{B} = \begin{bmatrix} 0 & 0 \\ 0 & 0 \\ 0 & 0 \\ -1 & 0 \\ 1 & 1 \end{bmatrix} \qquad \mathbf{F} = \begin{bmatrix} -1 & 0 \\ 0 & -1 \\ -1 & 0 \\ 0 & -1 \\ -1 & 0 \end{bmatrix} \qquad \mathbf{G} = \begin{bmatrix} -2 & 0 \\ -1 & -2 \\ 0 & 1 \\ -1 & 0 \\ 1 & -1 \end{bmatrix}.$$

With starting values of $\beta = 2$ and $\tau = 1$, tolerance of convergence $\varepsilon = 1e-12$, the program based on the algorithm described gave after 79 iterations the following solution

$$\beta = -2.9164 \qquad \tau = -46.5172\,.$$

This solution correspond to $\lambda = \pm 2.9164\mathrm{i}$ and the smallest positive time delay $\tau = 0.8809$.

3.7 Bisection - A Practical Approach

We now describe a practical numerically robust method which could be used to determine the entire stability boundary of the system. The method is applied to the transcendental eigenvalue problem (3.4), which we write for simplicity as

$$\left(\mathbf{E}(\lambda) - \mu(\lambda,\tau)\mathbf{H}(\lambda)\right)\mathbf{v} = \mathbf{0} \tag{3.61}$$

where

$$\mathbf{E}(\lambda) \equiv \lambda^2\mathbf{M} + \lambda\mathbf{C} + \mathbf{K}\,, \qquad \mathbf{H}(\lambda) = \mathbf{B}\left(\lambda\mathbf{F}^T + \mathbf{G}^T\right), \qquad \mu(\lambda,\tau) = e^{-\lambda\tau}\,. \tag{3.62}$$

For any given purely imaginary value of λ we may determine the eigenvalues $\mu(\lambda,\tau)$ in the generalized eigenvalue problem (3.61) by using a standard eigenvalue problem solver. The corresponding τ may then be determined via

$$\tau = -\frac{\ln\mu}{\lambda}\,. \tag{3.63}$$

In general the τ produced by (3.63) is expected to be complex. A physical solution corresponds to real τ. Hence by varying λ along a certain range on the imaginary axis we may determine a function $\tau(\lambda)$ where the physical solutions are characterized by $\mathrm{Im}(\tau)=0$. In MIMO systems $\mathrm{rank}(\mathbf{H})=m$ and there are m such functions corresponding to the m finite eigenvalues μ_k of (3.61). It should be noted that each μ_k generates via (3.63) an infinite set of time delays τ. However the elements in such an infinite set are different from each other by the real part only, while the imaginary part is the same. It thus follows that the function $\mathrm{Im}(\tau_k)$ is *uniquely* determined. Moreover, by the continuity of the eigenvalue μ with respect to the system's parameters the function $\mathrm{Im}(\tau)$ is *continuous*. By plotting $\mathrm{Im}(\tau)$ versus λ we may visualize the physical solutions which coincide with the roots.

To determine the actual value of a single physical solution within the interval $[\vec{\lambda},\overleftarrow{\lambda}]$ we may use a bisection strategy applied to the multiple continuous functions, $\mathrm{Im}(\tau_k)$, $k=1,2,...,m$. The criterion for the interval $[\vec{\lambda},\overleftarrow{\lambda}]$ to include a single solution is

$$\prod_{k=1}^{m}\mathrm{Im}(\vec{\tau}_k)\mathrm{Im}(\overleftarrow{\tau}_k)<1, \tag{3.64}$$

where $\vec{\tau}_k$ and $\overleftarrow{\tau}_k$ are the time delays at the boundaries of $[\vec{\lambda},\overleftarrow{\lambda}]$. The non-classical criterion (3.64) is advised to circumvent the elaborated process of pairing the time delays at one end of $[\vec{\lambda},\overleftarrow{\lambda}]$ with their counterparts at the other end of the interval. If the criterion (3.64) is not met, then there is no *single* root within the tested interval.

This approach is illustrated by the following example.

Example 3.7

We analyze the system of Example 3.6. For this case where $m=2$ the eigenvalue problem (3.61) has two finite eigenvalues for any chosen λ. Each eigenvalue leads via (3.63) to a time delay denoted by τ_1 and τ_2. We change λ along the imaginary axis in the interval $[0,6i]$ and obtain the functions $\tau_1(\lambda)$ and $\tau_2(\lambda)$. The imaginary parts of these functions are shown in Figure 3.3.

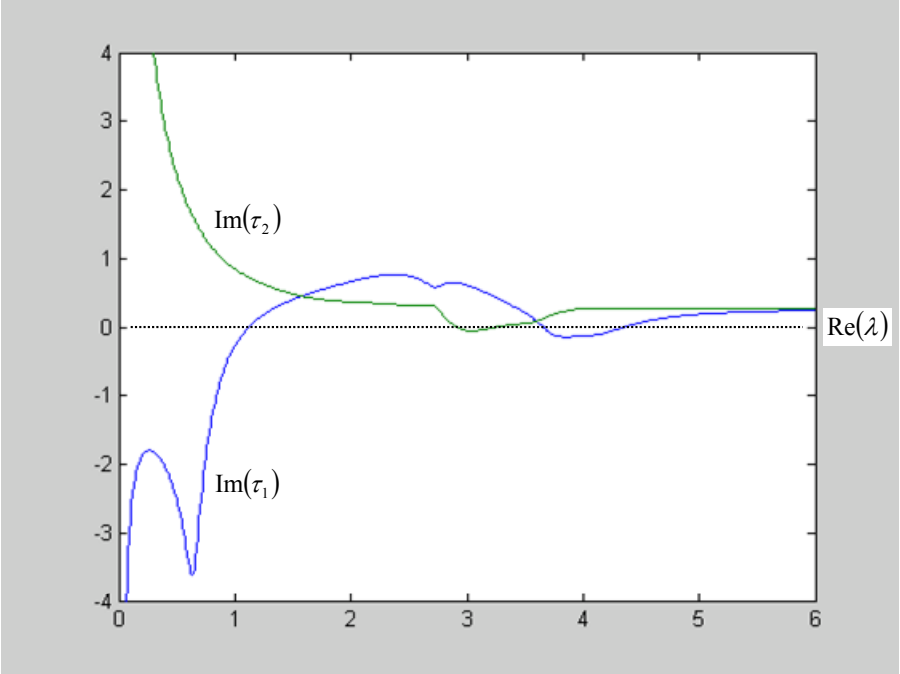

Figure 3.3 Graphs of the imaginary part of τ_k for λ in the interval $(0, 6i)$

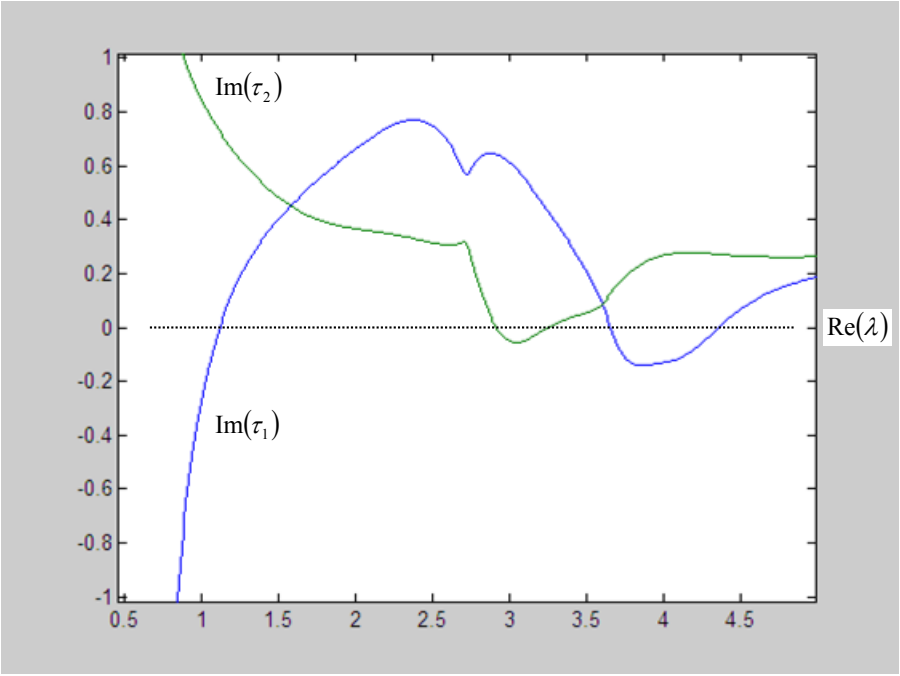

Figure 3.4 Zoom on the domain containing the roots of the graphs of Figure 3.3

It is clearly visualized from Figure 3.4 that there are five vanishing points which define initial boundaries for root-finding by the bisection method. We used the initial intervals,

$$[0.5 \quad 1.5], \qquad [2.5 \quad 3], \qquad [3 \quad 3.5], \qquad [3.5 \quad 4], \qquad [4 \quad 4.5],$$

and located the five solutions of λ_k and their corresponding τ_k shown in Table 3.2. Figure 3.4 zooms on the interval containing the roots of the functions.

Table 3.2 Critical time delays and their associated purely imaginary eigenvalues.

k	1	2	3	4	5
λ_k	1.1192i	2.9164i	3.2511i	3.6573i	4.3572i
τ_k	0.8804	0.8809	0.4293	1.4647	0.6702

The solution found in Example 3.6 is that of λ_2, τ_2 in the table.

3.8 Concluding Remarks

The boundaries of stability for SIMO controlled systems have been determined explicitly by the roots of a certain polynomial that we explained how to find. For MIMO controlled system we have transformed the problem into one of finding repeated roots of a certain equation. In the numerical method implementing Newton's iteration scheme, it was shown that the Jacobian matrix associated with the problem is singular in the neighborhood of the solution leading to linear convergence of the algorithm, rather than quadratic one. The bisection method applicable for multiple functions was advised. The method is practical and robust enough to characterize the complete stability boundary of mechanical control systems with time delay.

Chapter 4
Concluding Remarks and Future Work

4.1 Conclusions

The objective of this dissertation was to study the *boundary of stability of a mechanical system as a function of a parameter* and expand it to address some of the issues associated with mechanical system stability. Two different classes of systems were considered to elucidate the findings. The first system in Chapter 2, which is a double pendulum connected by a rigid rod moving in a plane, is a classical degenerate case of an uncontrolled undamped system. Linear perturbation and eigenvalue analyses are used in characterizing the behavior of the system. Chapter 3 investigates the critical time delays that an actively controlled mechanical system may lose or gain stability. Two variations, *a single-input/multi-output (SIMO) system* and a *multi-input/multi-output (MIMO) system* that follow the state feedback control law are considered.

The prime contributions of the results in Chapter 2 are:

- A zone of instability exists in what appears to be an inherently stable configuration of the double pendulum.
- The counterintuitive phenomenon of an asymmetric stable equilibrium for a symmetric system was revealed.
- The paradoxical behavior was explained mathematically and a simple experiment was designed to confirm the results.
- The results were extended to a chain of pendulums consisting of n masses and $n+1$ links, which was a lumped parameter model of a catenary.

The leading contributions of the results in Chapter 3 are:

- It was shown that, for a SIMO system, the problem of determining a closed form solution for the critical time delay maybe reduced using singular value decomposition (SVD) to one of finding the roots a certain polynomial.
- The technique however could not be exploited for polynomial reduction for the MIMO case. Two numerical methods, *Newton's iterations*, and *bisection for multiple functions*, are applied to analyze the stability for the MIMO case.

4.2 Recommendations for Future Work

The data as indicated in Table 2.1 shows that even for small values of $d < d_{CR}$, the instability in the system is substantial. There is a measurable change in the stable equilibrium configuration of the system subjected to infinitesimally small perturbations. This feature can be

harnessed practically to design sensing devices that indicate a change in system variables. The constrained pendulum investigated is the minimum model order required to formulate a discrete model of the catenary. Given the counterintuitive phenomenon that it has exposed, another plausible recommendation for future work would be to extend the results to higher dimensions and find the stability configurations in each case. Chapter 3 involves the determination of an analytical solution for the critical time delay of a SIMO system. The technique when extended to a MIMO system was challenged because of the size of matrices involved. An obvious recommendation would be to devise a method that renders a closed form solution for the time delay for a MIMO system as well.

References

E.I. Butikov, "On the dynamic stabilization of an inverted pendulum," *American Journal of Physics*, Vol. 69, pp. 755-768, 2001

L.H. Cadwell, E.R. Boyko, "Linearization of the simple pendulum," *American Journal of Physics*, Vol. 59, pp. 979-981, 1991

M. Maianti, S. Pagliara, G. Galimberti, F. Parmigiani, "Mechanics of two pendulums coupled by a stressed spring," *American Journal of Physics*, Vol. 77, pp. 834-838, 2009

M. Z. Rafat, M. S. Wheatland, T. R. Bedding, "Dynamics of a double pendulum with distributed mass," *American Journal of Physics*, Vol. 77, pp. 216-233, 2009

H. Ziegler, *"Principles of Structural Stability,"* (Blaisdell, London, 1968)

S.P. Timoshenko, J.M. Gere, *"Theory of Elastic Stability,*" (McGraw-Hill, London, 1961)

L. Meirovitch, *"Elements of Vibration Analysis,*" (McGraw-Hill, New York, 1986)

A.H. Nayfeh, *"Introduction to Perturbation Techniques,"* (Wiley-Interscience, New York, 1981)

H.M. Irvine, *"Cable Structures,"* (MIT, Cambridge, MA, 1981)

I.G. Tadjbakhsh, Y.M. Wang, "Transient vibrations of a taut inclined cable with a riding accelerating mass," *Nonlinear Dynamics*, Vol. 6, pp. 143-161, 1994

J.S. Chen, H.C. Li, W.C. Ro, "Slip-through of a heavy elastica on point supports," *International Journal of Solids and Structures*, Vol. 47, pp. 261-268, 2010

H.L. Langhaar, *"Energy Methods in Applied Mechanics,"* (Wiley, New York, 1962)

F.W. Sears, M.W. Zemansky, *"College Physics,"* 3rd Edition, (Addison-Wesley, London, 1960)

A. Cromer, "Many oscillations of a rigid rod," *American Journal of Physics*, Vol. 63, pp. 112-121, 1995

C.E. Smith, "Motions of a stretched string carrying a moving mass particle," *Journal of Applied Mechanics*, Vol. 31, pp. 29-37, 1964

H.M. Irvine, T.K. Caughey, "The linear theory of free vibrations of a suspended cables," *Proceedings of the Royal Society of London – Series A*., Vol. 341, pp. 299-315, 1974

J.D. Achenbach, C.T. Sun, "Moving load on a flexibly supported Timoshenko beam," *International Journal of Solids and Structures*, Vol. 1, pp. 353-370, 1965

Y.M. Ram, "A constrained eigenvalue problem and nodal and modal control of vibrating systems," *Proceedings of the Royal Society of London Series A – Mathematical, Physical and Engineering Sciences*, Vol. 466, pp. 831-851, 2010

R.P. Feynman, R.B. Leighton, M. Sands, *"The Feynman Lectures on Physics,"* (Pearson/Addison-Wesley, San Francisco, CA, 2006)

H. Goldstein, *"Classical Mechanics,"* 2nd Edition, (Addison-Wesley, Reading, MA, 1980)

S.D. Brierley, J.N. Chiasson, E.B. Lee, S.H. Zak, "On stability independent of delay for linear systems," *IEEE Transactions on Automatic Control*, Vol. 27, pp. 252-254, 1982

K. Gu, V.L. Kharitonov, J. Chen, *"Stability of time delay systems,"* (Birkhauser, Boston, 2003)

H.Y. Hu, Z.H. Wang, *"Dynamics of Controlled Mechanical Systems with Delayed Feedback,"* (Springer, Berlin, 2002)

E.W. Kamen, "On the relationship between zero criteria for two-variable polynomials and asymptotic stability of delay differential equations," *IEEE Transactions on Automatic Control*, Vol. 25, pp. 983-984, 1980

T. Mori, "Criteria for asymptotic stability of linear time-delay systems," *IEEE Transactions on Automatic Control*, Vol. 30, pp. 158-161, 1985

N. Olgac, R. Sipahi, "An exact method for the stability analysis of time-delayed linear time-invariant systems," *IEEE Transactions on Automatic Control*, Vol. 47, pp. 793-797, 2002

Y.M. Ram, "A method for finding repeated roots in transcendental eigenvalue problems," *Proceedings of the Institution of Mechanical Engineers, Part C, Journal of Mechanical Engineering Science*, Vol. 222, pp. 1665-1671, 2008

J.H. Su, "Further results on the robust stability of linear systems with a single time-delay," *Systems and Control Letters*, Vol. 23, pp. 375-379, 1994

J.H. Su, "The asymptotic stability of linear autonomous systems with commensurate time delays," *IEEE Transactions on Automatic Control*, Vol. 40, pp. 1114-1117, 1995

A. Thowsen, "Delay independent asymptotic stability of linear systems," *IEEE Proceedings D. Control Theory and Applications*, Vol. 129, pp. 73-75, 1982

A. Thowsen, "Stability of Time-Delay systems," *Further Comments, IEEE Transactions on Automatic Control*, Vol. 28, pp. 935-935, 1983

K. Walton, J.E. Marshall, "Direct method for TDS stability analysis," *IEEE Proceedings D. Control Theory and Applications*, Vol. 134, pp. 101-107, 1987

A. Singh, *"State Feedback Control with Time Delay,"* Dissertation, Louisiana State University, 2009

R.D. Driver, *"Ordinary and Delay Differential Equations,"* (Springer, New York, 1977)

J.K. Hale, *"Theory of Functional Differential Equations,"* (Springer Verlag, New York, 1977)

V.B. Kolmanovski, V.R. Nosov, *"Stability of Functional Differential Equations,"* (UK: Academic, London, 1986)

M.J. Satche, "Stability of linear oscillating systems with constant time lag," *Journal of Applied Mechanics*, Vol.16, pp. 419-420, 1949

A.D. Dimarogonas, S. Haddad, *"Vibration for Engineers,"* (Prentice-Hall, New Jersey, 1992)

J.E. Mottershead, Y. M. Ram, "Inverse eigenvalue problems in vibration absorption: Passive modification and active control," *Mechanical Systems and Signal Processing*, Vol. 20 (1), pp 5-44, 2006

J.E. Mottershead, M. G. Tehrani, D. Stancioiu, S. James, H. Shahverdi, "Structural modification of a helicopter tailcone," *Journal of Sound and Vibration*, Vol. (1-2), pp 366-384, 2006

H.W. Turnbull, *"Theory of Equations,"* (Oliver and Boyd, Edinburgh, 1947)

Vita

Prashanth Ramachandran was born in Madurai, India. He completed his schooling from TVS School, Madurai. He joined Anna University, Chennai, India, in 2002 and earned a Bachelor of Engineering degree in Mechanical Engineering in May 2006. After his graduation, he worked with TVS Sundram Fasteners, Hosur, India as a Design & Development Engineer for a year. Following this, he embarked on his graduate program in the fall of 2007 and graduated with a Master of Science in Mechanical Engineering in May 2009 from Louisiana State University. He joined the Doctoral program in the Department of Mechanical Engineering in the spring of 2009. He started working full-time in August 2010 with Hanna Cylinders, Libertyville, as a Research & Development Engineer. Prashanth will graduate with his Doctor of Philosophy degree in Mechanical Engineering in August 2012 and pursue a consulting career in the field of mechanics and vibration.